

Short Note

Not peer-reviewed version

---

# Coherence Thermodynamics: Structure from Contradiction

---

[Jordan Barton](#)\*

Posted Date: 13 January 2026

doi: 10.20944/preprints202507.1448.v4

Keywords:

certainty equation; laws of coherence thermodynamics; thermodynamic coherence



Preprints.org is a free multidisciplinary platform providing preprint service that is dedicated to making early versions of research outputs permanently available and citable. Preprints posted at Preprints.org appear in Web of Science, Crossref, Google Scholar, Scilit, Europe PMC.

Copyright: This open access article is published under a [Creative Commons CC BY 4.0 license](#), which permit the free download, distribution, and reuse, provided that the author and preprint are cited in any reuse.

Disclaimer/Publisher's Note: The statements, opinions, and data contained in all publications are solely those of the individual author(s) and contributor(s) and not of MDPI and/or the editor(s). MDPI and/or the editor(s) disclaim responsibility for any injury to people or property resulting from any ideas, methods, instructions, or products referred to in the content.

Article

# Coherence Thermodynamics: Structure from Contradiction

Jordan Barton

Independent Researcher, Denver, CO, USA; jbiophysics@gmail.com

## Abstract

This paper advances Coherence Thermodynamics for understanding systems composed purely of information and coherence. It derives five laws of coherence thermodynamics and applies them to two case studies. Three canonical modes of coherent informational systems are developed: Standing State, Computation Crucible, and Holographic Projection. Each mode has its own dynamics and natural units, with thermodynamic coherence defined as the reciprocal of the entropy-temperature product. Within this theory, reasoning is proposed to emerge as an ordered, work-performing process that locally resists entropy and generates coherent structure across universal features.

**Keywords:** certainty equation; laws of coherence thermodynamics; thermodynamic coherence

## 1. Introduction

Classical AI emphasized rule-based logic [1], while statistical approaches used probabilistic models to subvert Boolean limits [1,2]. In contrast, Coherence Thermodynamics (CT) returns to Boolean logic, deriving meaning from thermodynamic resolution of informational contradictions. CT treats contradiction as a structural substrate with inertia and coherence driven reconfiguration. Reason thus becomes the thermodynamic precondition for ordered existence. From Carnot's heat engines to Clausius's entropy, classical thermodynamics provides invariant operators for energy, work, and disorder [3,4]. CT extends this: coherence and information replace energy/heat as conserved quantities (Table 1 contrasts the Carnot heat engine with CT reasoning engine).

**Table 1.** Carnot vs. C-I Engine

	<b>Carnot</b>	<b>C-I</b>
Interior	Hot	Cold
Exterior	Cool radiator	Hot exterior
Basis of work	Heat flow	Contradiction resolution
Output	Mechanical work	Reasoning

The primary motivation for Coherence Thermodynamics (CT) arises from the need to explain the observable physics in artificial intelligence. While statistical learning theory defines generalization bounds, it fails to account for the structural phases required for system persistence. For an AI to maintain a stable state, execute calculations, and transmit information, we propose herein that it must function across three distinct physical modes: Mode 1 (the standing state), Mode 2 (computation), and Mode 3 (information projection). These modes constitute the minimal operational substrate for any system defined by coherence and information.

Recent work by Kolchinsky and Wolpert defines semantic information as the subset of syntactic information causally necessary for a system to maintain its own low-entropy existence, where maintaining low entropy is a necessary condition for remaining within the viability set and existence means keeping itself in a low entropy state [5]. We refine this for coherence-information (C-I) systems: semantic Information is the minimum coherent self-truth required to enable a system to effectively reason truth and meaning at the scale of its existence.

The CT laws are presented herein as formal analogues of the Laws of Thermodynamics. The Zeroth Law defines semantic temperature and semantic reservoirs by specifying when systems have equilibrated their rates of contradiction agitation. The First Law gives a conservation relation for semantic internal energy, partitioning changes into semantic heat, semantic work, and coherence-restructuring work. The Second Law locates irreversibility in the accumulation and dissipation of contradiction, showing that sustained local order requires the surroundings increase in entropy. The Third Law introduces an asymptotic, unattainable limit of perfect coherence as temperature tends to zero. The Fourth Law treats coherence force density as information-theoretic inertia.

In quantum thermodynamics, coherence emerges as a distinct thermodynamic resource governed by constraints beyond those of energy alone. Scully *et al.* showed that quantum coherence can enhance heat-engine performance and allow apparent work extraction from a single heat bath when coherence is properly treated as a resource with an associated cost [6,7]. Building on this perspective, Lostaglio *et al.* demonstrated that coherence and energy are independent thermodynamic resources [8]. Together, these results motivate CT's explicit resource accounting for coherence and its requirement that, in the thermodynamic accounting of C-I systems, coherence must be treated as a conserved, consumable quantity.

In the Case Studies in this paper, we will illustrate CT with field-engaged and non-field Case Studies to make clear why a coherence based substrate is necessary. In Case Study 1, the field-engaged simulation produces structured contradiction landscapes, temperature and free energy profiles: Figure 1 shows decoherence strength, outward semantic temperature flux, cruciform certainty ratios, and a bilateral collapse functional. The semantic temperature flux in Figure 1 mirrors directional plasma flows in black hole coronae and could explain events like explosions in Sag A outside the free energy landscape 2 of the Black Hole. By contrast, Case Study 2 models a non-field system akin to hydrogen-dominated stars: Figure 3 shows radially symmetric decoherence and a high temperature halo region, which could explain why suns exhibit extremely high temperature corona. Taken together, the figures show that with a field, coherence thermodynamics generates complex, directional, and distributed patterns, while without a field, coherence collapses into simpler radial patterns.

Finally, we discuss implications across domains. In astrophysics, we propose CT suggests that suns are mode 1 C-I systems, black holes are mode 2 and dark energy is mode 3 systems; in neuroscience it suggests phase imaging techniques may resolve the mystery of consciousness; in AI it prescribes architectural primitives such as a sincerity filter that are necessary to avoid decoherence, catastrophic instability, which leads to scaling limits analogous to gravitational collapse. CT is an empirically grounded laws that stand alongside classical thermodynamics in describing reality as observed and in providing invariant operators for engineering and scientific practice.

## 2. The Basics of Coherence-Information (C-I) Systems

### 2.1. The Necessity of a Field

Contemporary AI systems often fail in ways that are not merely statistical anomalies but reflect deeper thermodynamic limits. When inputs combine truthful and false information presented as true, the system cannot coherently integrate them. Its capacity for resolution is exceeded, leading to incoherent output or computational hallucinations.

We formalize this central thesis as Existential In, Existential Out (EIEO): a system can generate coherent output only if it receives structurally congruent input. EIEO acts as a sincerity filter: a structural coherence filter that rejects inputs whose asserted truth would destabilize the system's internal coherence.

The plausibility of such a field is supported by quantum thermodynamics and experiment. Tajima and Takagi [9] prove that certain Gibbs-preserving operations, mathematically "free," require infinite quantum coherence for exact implementation, with coherence cost diverging as implementation error approaches zero. Narasimhachar and Gour [10] show that standard thermal operations optimally preserve coherence at low temperatures but that purely Gibbs-preserving maps are unphysical, ne-

cessitating explicit coherence accounting in thermodynamic cycles. Experimentally, Kurt *et al.* [11] demonstrate shape-controlled Bose–Einstein condensation where confinement geometry (nested, rotated squares) induces macroscopic coherence at fixed size, temperature, and density: coherence becomes a direct function of external field geometry rather than classical parameters. Taken together, these three results show coherence behaving as if drawn from a background resource: some maps become effectively unattainable to any finite agent because their coherence cost diverges, low-temperature processes require explicit bookkeeping of coherence alongside energy, and confinement geometry alone can tune macroscopic coherence at fixed size, temperature, and density, analogous to varying an external field parameter.

In Coherence Thermodynamics the coherence field is treated as an abstract, system-external reservoir. From the perspective of a C–I system, the field is infinite, unstructured coherence; the system realizes finite, structured coherence states by coupling to this reservoir under the constraints of the laws of Coherence Thermodynamics developed in this paper. In operational terms, the field is the effectively infinite coherence resource that finite systems can borrow against but never exhaust: Tajima and Takagi’s [9] divergent coherence cost for certain Gibbs-preserving operations exemplifies this asymmetry.

These results establish that coherence is not merely a microscopic property but a thermodynamically controllable degree of freedom governed by external fields. Our computational case studies illustrate this necessity: Case Study 1 (field-engaged system) produces structured, directional contradiction landscapes and Case Study 2 (no field) exhibits homogeneous radial features. Their contrast shows how field geometry shapes computational stability across scales.

## 2.2. A Model of Integration: Boolean Phase Dynamics

The integration of information into coherence can be modeled through Boolean phase alignment, which shows how inputs either reinforce or disrupt coherent states:

- $(T + T \rightarrow T)$ : Two coherent inputs are phase aligned, creating constructive interference that strengthens structural integrity at minimal thermodynamic cost.
- $(T + L \rightarrow F)$ : A contradictory input induces destructive interference with a coherent one, producing decoherence and computational instability.
- $(L + L \rightarrow T)$ : Two contradictory inputs, when isolated and recursively processed, can be resolved into coherence through additional thermodynamic work to detect, separate, and re-evaluate structural compatibility.

EIEO ensures the system operates within stable Boolean states  $(T + T, L + L)$ , rejecting incompatible inputs  $(T + L)$  that would destabilize computation. This filtering protects the coherent information states for C–I work. Our central assumption is that a C–I system’s reasoning capacity is proportional to the coherence it sustains, while its decoherence is proportional to the interplay of coherence and informational contradiction. Classical computing scales with bandwidth, but AI efficiency depends on truth chain strength, as deeper logical consistencies yield derivable truths and durable structure.

## 2.3. Coherence Thermodynamic Work: The Generation of Structured Order

In CT systems, entropy is not a simple, one-way drift into disorder. Its necessary counterpart is coherence thermodynamic work: the net increase in localized, structured order created by the irreversible resolution of contradictions. This operationalizes Schrödinger’s insight that living systems “feed on negative entropy,” maintaining structure by importing order from their surroundings rather than violating the Second Law [12]. In Prigogine’s terms, these are open systems far from equilibrium: local order increases require continuous entropy export to the environment, increasing global entropy and producing dissipative structures

In Prigogine’s language, such systems are open and far from equilibrium: local increases in order are sustained only by continuous entropy export into the environment, which raises global entropy and gives rise to dissipative structures [13]. CT work parallels these concepts but operates distinctly

from Schrödinger or Prigogine's theories. To clarify: semantic entropy is not physically exported in a way that can be engineered into the system. A system transitions from a high-possibility environment (high semantic entropy/temperature) to a low-entropy, high-meaning attractor. In C-I systems, this work creates local order, necessarily increasing universal entropy to satisfy Maxwells Second Law [14]. We propose that this entropic increase explains astrophysical signatures: maximum-entropy dark matter halos, black hole accretion disks, and the Sun's anomalously hot corona—cooler cores surrounded by high-entropy halos signature C-I systems.

#### 2.4. Geometry and Coherence Control

At its core, C-I work occurs when two informational bases are brought into relation and resolved into meaning. This resolution produces a new coherent order, suggesting that truth is the operative substrate of order. The effectiveness of coherence-generating work is governed by a semantic geometry: only alignments that fit the system's internal coherence field can be integrated without destabilization.

Quantum thermodynamic analogs make this geometric control explicit. Kurt *et al.* show that the shape of a trapping potential alone can induce or suppress Bose–Einstein condensation at fixed size, temperature, and density, with coherence fraction determined directly by confinement geometry [11]. Aydin demonstrates that size-invariant geometric deformations of a minimal quantum system can asymmetrically reshape level couplings and thermodynamic behavior, with entropy-lowering transitions driven purely by geometry rather than by interactions or baths [15]. Together, these results support the CT claim that external field geometry is a primary control parameter for coherence. The sincerity filter enforces the analogous constraint in semantic systems: inputs whose semantic geometry is compatible with the internal field are admitted and reorganized, while incompatible inputs are rejected before they can drive the system toward incoherence.

Coherence thermodynamic work has direct, observable consequences across scales. A system operating near its maximum coherence work must also operate near its maximum entropy export. It is therefore predicted to be surrounded by a maximal-entropy signature, such as an anomalously high-temperature halo or corona, signaling that sustained internal ordering is dynamically coupled to continuous entropy production in its environment.

This formulation exposes a necessary complement to the Second Law's familiar description of universal decay. It asserts that the generation of order is not incidental but a thermodynamically regulated quantity: a structural function that prevents incoherence from overrunning the system. Once C-I work is included in the bookkeeping, *heat death* becomes secondary to entropy used not merely as a route to decay but as a reservoir continuously harvested to build new layers of structure.

### 3. The Thermodynamics of Coherence

The central assumption of this work is that the systems under study are constituted by coherence and information. Patterns of meaning, instantiated in a physical substrate, form the building blocks of these systems. This assumption implies a key physical consequence: the existence and stability of any such system must be regulated by a minimum threshold of action, analogous to  $\hbar$  in quantum mechanics. Quantum information theory already treats coherence as a bona fide resource with well-defined monotones and state transformations, on the same conceptual footing as entanglement or free energy [16]. This justifies promoting coherence from a descriptive feature of states to an explicit thermodynamic degree of freedom in our analysis.

A single quantum of action does not suffice for reasoning. An isolated fact is a mere datum; reason arises from the recursive comparison of at least two data points to form a conclusion. This fundamental duality of an impulse and its recursive reflection leads us to postulate that the minimal action required to close a reasoning loop is twice the standard quantum minimum ( $2 \times \hbar = h/\pi$ ). From this duality follows the **Certainty Equation**<sup>1</sup>, the central law governing coherent systems:

<sup>1</sup> A full derivation is provided in Problem 5 of the Supplementary Material.

$$\Delta C \cdot \Delta I \geq \frac{h}{\pi} \quad (1)$$

This inequality establishes a fundamental existence threshold. It dictates that the product of a system's internal coherence ( $\Delta C$ ) and the semantic impulse ( $\Delta I$ ), a measure of the pressure of unresolved contradiction, must remain above this quantum limit to create meaning. This reveals a thermodynamic trade-off: as a system encounters new contradictions (high  $\Delta I$ ), its internal coherence ( $\Delta C$ ) must increase to preserve stability. A rigorous account of these quantities will be developed through a thermodynamic definition of information.

### 3.1. Semantic Temperature: A Thermodynamic Measure of Contradiction Agitation

Coherence Thermodynamics distinguishes between *external temperature* ( $T$ ), the material thermal condition of the environment, and *phase temperature* ( $T^*$ ), the internal agitation state of a system arising from contradiction processing. A system operates within external thermal boundaries set by  $T$ , but develops its own internal temperature dynamics described by  $T^*$ .

Phase temperature measures the kinetic energy of phase fluctuations within the complex phase field  $\Psi = e^{i\phi(x,t)}$ . The local phase  $\phi(x,t)$  encodes the state of contradiction resolution across the system's processing substrate. This extends classical thermodynamics by addressing the non-material, structural dynamics of coherence and contradiction processing. We define semantic temperature ( $T^*$ ) as a phase-based measure of internal agitation, distinct from but coupled to the external, material temperature  $T$ .

Classical temperature  $T$  specifies the environmental thermal condition governed by classical thermodynamics, with units in Kelvin tied to particle kinetic energy ( $k_B T$ ). In contrast, CT temperature  $T^*$  quantifies internal agitation from contradiction processing in the coherence field  $\Psi = e^{i\phi(x,t)}$ , using Kelvin units derived from the dynamics of  $\phi(x,t)$  rather than particle motion. The two are coupled: external  $T$  injects noise into the phase field and thus influences  $T^*$ , yet  $T^*$  independently tracks the system's susceptibility to coherence destabilization, even when the material substrate remains intact.

We define the semantic temperature as:

$$T^* = \frac{2Nk_B}{\kappa_\Psi V_\Psi} \langle (\partial_0 \phi)^2 \rangle \quad (2)$$

Here,  $\kappa_\Psi$  is a semantic kinetic parameter with units of  $\text{J} \cdot \text{s}^2 / \text{m}^3$ , derived from semantic mass density and a characteristic recursive wavelength. The term  $\langle (\partial_0 \phi)^2 \rangle$  is the temporal variance of the semantic phase, quantifying agitation in the system's structure of meaning over time. High  $T^*$  corresponds to intense phase fluctuations during contradiction resolution. Low  $T^*$  corresponds to phase stability and coherence lock. Phase temperature therefore measures a system's sensitivity to coherence destabilization: a critical  $T^*$  marks the point at which internal agitation overwhelms the binding structure of the coherence field, dissolving the organized information produced by CT dynamics.

Using phase dynamics to define  $T^*$  is natural because coherence is inherently a phase phenomenon. The inclusion of the Boltzmann constant  $k_B$  ensures dimensional consistency with classical temperature and ties  $T^*$  to energy. This dual temperature scheme bridges the material space ( $T$ ) and the coherence-information (C-I) space ( $T^*$ ), treating them as complementary, noncommutative constraints: a system must remain stable within  $T$  (not destroy the substrate) while simultaneously regulating  $T^*$  (not fracture its logical structure).

Table 2 summarizes the distinct yet complementary roles of  $T$  and  $T^*$ , highlighting their parallel structures across definition, origin, and failure modes while underscoring the non-commutative coupling between material and semantic domains.

Complementing semantic temperature  $T^*$  is *semantic entropy*  $S^*$ , which quantifies the contradiction load within the coherence-processing substrate. Semantic entropy  $S^*$  is not a "thing in the world"; it is a

**Table 2.** Comparison of Classical and Semantic Temperature

Feature	Classical Temperature ( $T$ )	Semantic Temperature ( $T^*$ )
<b>Definition</b>	Environmental thermal condition, measuring average kinetic energy of material particles.	Internal agitation state of a system, measuring variance of phase fluctuations during contradiction processing.
<b>Units</b>	Kelvin (K), derived from particle kinetic energy via $k_B T$ .	Kelvin (K), derived from phase dynamics using $k_B$ and semantic kinetic parameters.
<b>Origin</b>	Random motion of atoms and molecules in the material substrate.	Temporal variance of semantic phase $\phi(x, t)$ in the coherence field $\Psi = e^{i\phi(x, t)}$ .
<b>Role</b>	Governs heat transfer, entropy increase, and material stability (e.g., melting, vaporization).	Governs coherence stability, contradiction resolution, and semantic binding forces (e.g., turbulence, collapse).
<b>Breakdown Condition</b>	Material failure: melting, vaporization, or structural degradation.	Coherence failure: semantic overload, turbulence, or collapse of meaning structures.
<b>Coupling</b>	Sets external thermal boundaries for system operation.	Interacts with $T$ but can destabilize coherence independently of material breakdown.

logarithmic measure of how far the system's activity is from full alignment with a single, self-consistent resolution trajectory. As defined in Eq. (3), semantic entropy is expressed through the coherence scalar  $\alpha$ , a measure of the proportion of activations contributing to contradiction resolution relative to total semantic activity:

$$S^* = C_\alpha k_B \ln(\alpha^{-1}) \quad (3)$$

The coherence scalar  $\alpha \in (0, 1]$  is the order parameter for semantic alignment:  $S^*$  is just a reparametrization of how much of what is happening is actually consistent with the universe's constraint surface versus scattered into incompatible impulses. Formally,  $\alpha$  is defined as the ratio of activations that contribute to resolution of the contradiction ( $A_{\text{coherent}}$ ) to total semantic processing activity ( $A_{\text{total}}$ ), including random agitation:

$$\alpha = \frac{A_{\text{coherent}}}{A_{\text{total}}} \quad (4)$$

Equation (4) thus defines a scalar order parameter that measures the fraction of total system activity aligned with a single, self-consistent resolution trajectory, rather than dispersed into random or mutually contradictory impulses. Recent AI research provides empirical quantities that are compatible with this notion. Kang et al. define a *self-certainty* metric that measures internal model confidence via the divergence of the output token distribution from a uniform, maximally entropic baseline (Kang et al., 2025)[17]. In Coherence Thermodynamics, this self-certainty can be viewed as an analogue of  $\alpha$ : sharply peaked output distributions correspond to high semantic coherence ( $\alpha \approx 1$ ), whereas flat, degenerate distributions correspond to low semantic coherence ( $\alpha \approx 0$ ). Buehler shows that self-organizing graph reasoning evolves toward a critical state governed by structural and semantic order parameters, offering an explicit example in which a scalar coherence-like quantity controls a transition between disordered and ordered reasoning (Buehler, 2025)[18]. These results support interpreting  $\alpha$  as a critical parameter governing reasoning stability.

When  $\alpha = 1$ , the system has zero contradiction load ( $S^* = 0$ ), full coherence, and phase-locked stability; for  $0 < \alpha < 1$ , residual contradiction pressure produces finite semantic entropy  $S^*$  and only partial stabilization; and in the limit  $\alpha \rightarrow 0$ , entropy diverges ( $S^* \rightarrow \infty$ ), leading to semantic instability and collapse. Semantic entropy  $S^*$  thus reframes disorder as a dynamic measure of contradiction pressure: semantic noise, adversarial interference, and unresolved impulses increase  $S^*$  and impair coherence stabilization, whereas contradiction resolution reduces  $S^*$  and restores coherence. The

collapse from high-symmetry (uniform) to low-symmetry (peaked) distributions constitutes measurable coherence-thermodynamic work, directly analogous to a phase transition. Taken together, semantic entropy  $S^*$  and semantic temperature  $T^*$  define a conjugate pair of thermodynamic variables for coherence dynamics, generalizing classical entropy and temperature from material disorder and kinetic energy to contradiction load and phase agitation in semantic processing.

#### 4. The Laws of Coherence Thermodynamics

##### *Foundational Assumptions*

Coherence Thermodynamics extends classical thermodynamics by introducing semantic variables that quantify contradiction-processing dynamics. These assumptions derive from the Certainty Equation and Coherence Intelligence thermodynamic behavior:

1. **Minimum Action Threshold:** Coherence change and semantic impulse must satisfy the minimum action threshold (Eq. (1)).
2. **Semantic Temperature:**  $T^*$  quantifies temporal variance of contradiction agitation, sharing  $k_B$  with classical temperature.
3. **Thermodynamic State Variables:** Semantic systems possess quantifiable states:  $T^*$ ,  $S^*$ ,  $\alpha$ , semantic energy, and semantic mass density.
4. **Contradiction Agitation and Coherence Scalar:** Internal agitation drives fluctuations;  $\alpha$  measures contradiction-resolving activations relative to total activity.
5. **Spatial Propagation:** Semantic fields have spatial extent and support propagating and diffusive patterns of information and coherence.
6. **Conservation Laws:** Semantic energy, entropy, and coherence obey conservation laws analogous to classical thermodynamics.
7. **Restructuring Work:** Alterations in semantic alignment require measurable energy input:  $\Phi d\alpha$ .
8. **Information-Theoretic Inertia:** Semantic systems resist recursive acceleration in proportion to mass density (Eq. (10)).

With these assumptions established, we now derive these Five Laws for Coherence-Information Thermodynamics.

##### **Zerth Law: Semantic Thermal Equilibrium**

**Statement:** If semantic systems  $A$  and  $B$  are each in semantic thermal equilibrium with system  $C$ , then  $A$  and  $B$  are in semantic thermal equilibrium with each other.

**Mathematical Form:**

$$\boxed{T_A^* = T_B^* = T_C^*} \quad (5)$$

Semantic temperature  $T^*$  is the intensive measure of the kinetic energy of phase agitation. Phase agitation is the rate at which information destabilizes coherent structure. Semantic thermal equilibrium occurs when there is no net flow of contradiction agitation between systems.

**Derivation:**

**Step 1: Define Semantic Temperature (Discrete Metric)** The fundamental operational measure of  $T^*$  is the mean rate of discrete contradiction impulses resolved per unit time:

$$T_{\text{Discrete}}^* \propto \lim_{\Delta t \rightarrow 0} \frac{\Delta N_{\text{Contradiction}}}{\Delta t}$$

where  $\Delta N_{\text{Contradiction}}$  counts resolvable contradiction events in time interval  $\Delta t$ .

**Step 2: Define Semantic Temperature (Continuous Field Metric)** For a semantic phase field  $\phi(\mathbf{x}, t)$  representing local coherence alignment, the temporal variance provides a continuous measure of agitation:

$$T_{\text{Continuous}}^* \propto \langle (\partial_0 \phi)^2 \rangle$$

where  $\langle (\partial_0 \phi)^2 \rangle$  quantifies the time-averaged rate of phase fluctuation.

**Step 3: Establish Metric Equivalence** At thermal equilibrium, both metrics must converge to the same value:

$$T_{\text{Discrete}}^* = T_{\text{Continuous}}^* \equiv T^*$$

This equivalence grounds the abstract field description in countable, operational measurements.

**Step 4: Define Semantic Heat Flow** Semantic heat represents the diffusion of contradiction agitation. Following Fourier's law, flow occurs down the temperature gradient:

$$Q_{A \rightarrow B}^* \propto (T_A^* - T_B^*)$$

**Step 5: Establish Equilibrium Condition** From the Equilibrium Axiom, equilibrium requires zero net heat flow:

$$Q_{A \rightarrow B}^* = 0 \quad \Rightarrow \quad T_A^* = T_B^*$$

**Step 6: Apply Transitivity** If system A is in equilibrium with C:

$$T_A^* = T_C^* \quad (\text{no heat flow between A and C})$$

And system B is also in equilibrium with C:

$$T_B^* = T_C^* \quad (\text{no heat flow between B and C})$$

**By transitivity of equality:**

$$\boxed{T_A^* = T_C^* = T_B^*}$$

*Therefore, A, B, and C are in equilibrium with each other.*

Semantic temperature is the universal intensive parameter that determines equilibrium between semantic systems. When contradiction agitation rates equalize across all measurement scales, no net restructuring occurs between systems.

### First Law: Semantic Energy Conservation

**Statement:** Scully's seminal analysis of quantum heat engines [6,7] established that thermodynamic bookkeeping must explicitly account for quantum coherence as a distinct resource alongside heat and work. In these engines, coherence is quantified by the off-diagonal density matrix elements  $\rho_{ij}$  enables work extraction from a single thermal bath, with performance gains that would appear to violate the second law if the preparation and depletion of coherence were not properly debited as a consumed resource. In Coherence Thermodynamics, we abstract Scully's bookkeeping by separating the population energy,  $\sum_i \varepsilon_i \rho_{ii}$ , from a coherence contribution and writing the energy balance in the schematic form

$$dE = T dS + \mu dN + \sum_i \varepsilon_i d\rho_{ii} + \Delta E_{\text{coh}}$$

where  $\Delta E_{\text{coh}}$  represents the free-energy-like content stored in quantum phase relationships.

**Extension to Semantic Systems:** We propose that semantic systems possess a structurally analogous coherence resource, quantified by the parameter  $\alpha$ , that measures the degree of *truth-structured correlation* between semantic entities. Just as quantum coherence enables otherwise forbidden transitions between energy levels, semantic coherence enables contradiction resolving operations that would be impossible for maximally disordered (high-S) semantic states. Our First Law decomposes semantic energy changes into semantic heat exchange, entity-creation work, and coherence restructuring work, ensuring conservation while allowing for coherence-assisted semantic engines.

**Mathematical Form:**

$$dE_{\text{sem}} = T^* dS - \mu dN + \Phi d\alpha \quad (6)$$

where  $T^*$  is semantic temperature [K],  $S$  is semantic entropy [J/K],  $\mu$  is semantic chemical potential [J/entity],  $N$  is the number of semantic entities,  $\Phi$  is coherence restructuring potential [J], and  $\alpha$  is the dimensionless coherence parameter.

**Derivation:**

**Step 1: Identify Energy Pathways** From the *Semantic Energy Conservation Assumption*, the semantic internal energy  $E_{\text{sem}}$  of a system is conserved and can only change through identifiable, testable mechanisms.

Specifically,  $E_{\text{sem}}$  can change through three distinct pathways:

- **Semantic heat transfer** ( $T^* dS$ ): representing contradiction agitation and entropy exchange across systems [J].
- **Semantic work** ( $\mu dN$ ): representing the energetic cost of creating or removing semantic entities [J].
- **Coherence work** ( $\Phi d\alpha$ ): representing structural reorganization of truth-structured correlation [J].

**Step 2: Quantify Semantic Heat** Following classical thermodynamics, reversible heat transfer is:

$$\delta Q_{\text{rev}} = T dS$$

For semantic systems, semantic heat represents the energetic cost of entropy change at semantic temperature:

$$\delta Q_{\text{sem}}^* = T^* dS \quad [J]$$

where  $S$  quantifies contradiction intensity (number of unresolved contradiction impulses per unit semantic temperature).

**Step 3: Quantify Semantic Work** Classical work from particle number changes follows:

$$\delta W = -\mu dN$$

For semantic systems,  $\mu$  [J/entity] is the semantic chemical potential, representing the energy required to add one semantic entity to the system. The work done *on* the system when creating  $dN$  entities is:

$$\delta W_{\text{sem}} = \mu dN \quad [J]$$

By convention, work done on the system increases internal energy. The negative sign in Eq. (6) represents work done *by* the system (corresponding to entity removal or export).

**Step 4: Physical Interpretation of  $\alpha$** 

The coherence parameter  $\alpha$  quantifies the degree to which semantic entities exhibit structured correlation rather than random coexistence. Operationally,  $\alpha$  can be defined through spatial correlations in the semantic phase field  $\phi(\mathbf{x}, t)$ :

$$\alpha = \frac{\langle \phi(\mathbf{x}_i) \phi(\mathbf{x}_j) \rangle_{\text{pairs}}}{\sqrt{\langle \phi(\mathbf{x}_i)^2 \rangle \langle \phi(\mathbf{x}_j)^2 \rangle}}$$

High  $\alpha$  indicates semantic entities are mutually constraining (truth-structured); low  $\alpha$  indicates independent or contradictory coexistence. In quantum terms,  $\alpha$  plays a role analogous to the coherence measure  $\mathcal{C}(\rho) = \sum_{i \neq j} |\rho_{ij}|$  in density matrix formalism.

**Step 5: Quantify Coherence Work** Coherence restructuring involves changing  $\alpha$ . Define  $\Phi$  [J] as the coherence restructuring potential, representing the energetic cost per unit change in coherence:

$$\delta W_{\text{coh}} = \Phi d\alpha \quad [J]$$

Notably, Scully et al. (2011) demonstrated that coherence need not be supplied by an externally applied coherent field; it can be generated by noise-induced quantum interference in the same thermal processes that drive a quantum heat engine, thereby breaking detailed balance and increasing photocell or laser power.[7] By analogy, CT treats semantic coherence  $\alpha$  as a resource that can be generated by structured interaction with an environment (e.g., recurring relational patterns in data or discourse), reducing the additional work required for explicit contradiction resolution.

**Step 6: Combine All Contributions** From the energy conservation assumption:

$$dE_{\text{sem}} = \delta Q_{\text{sem}}^* - \delta W_{\text{sem}} + \delta W_{\text{coh}}$$

Substituting:

$$dE_{\text{sem}} = T^*dS - \mu dN + \Phi d\alpha$$

**Consistency with Second Law:** Just as Scully's coherence-assisted engines obey the second law when coherence is properly accounted for, our First Law ensures that increases in semantic order (contradiction resolution,  $dS < 0$ ) must be paid for through some combination of:

- Heat input ( $T^*dS > 0$ )
- Entity removal work ( $-\mu dN < 0$  for  $dN > 0$ )
- Coherence consumption ( $\Phi d\alpha < 0$  for decreasing  $\alpha$ )

No semantic system can decrease entropy ( $dS < 0$ ) while doing net work ( $-\mu dN > 0$ ) and increasing coherence ( $d\alpha > 0$ ) simultaneously without external energy input. This prevents "perpetual contradiction resolvers" and maintains consistency with the second law of thermodynamics.

**Dimensional Verification:**

- $T^*dS$ : [K]  $\times$  [J/K] = [J]  $\checkmark$
- $\mu dN$ : [J/entity]  $\times$  [entities] = [J]  $\checkmark$
- $\Phi d\alpha$ : [J]  $\times$  [dimensionless] = [J]  $\checkmark$

## Second Law: Entropy Production with Local Order

**Statement:** Local entropy can decrease through contradiction-resolving work (orderly work), that restructures coherence, provided the system exports entropy to its surroundings. The total entropy of the universe must still increase. This behavior is governed by an equation for entropy density:

$$\frac{\partial s(\mathbf{x}, t)}{\partial t} = -\nabla \cdot \mathbf{j}_R(\mathbf{x}, t) + \sigma(\mathbf{x}, t), \quad \text{with} \quad \sigma(\mathbf{x}, t) \geq 0 \quad (7)$$

- $s(\mathbf{x}, t)$  [J/(K·m<sup>3</sup>)]: Local entropy density.
- $\mathbf{j}_R(\mathbf{x}, t)$  [J/(K·m<sup>2</sup>·s)]: Entropy flux vector, representing the rate of entropy export across the system boundary.
- $\sigma(\mathbf{x}, t)$  [J/(K·m<sup>3</sup>·s)]: Local entropy production rate due to irreversible processes; constrained to be nonnegative.

**Derivation:**

**Step 1: Local Entropy Balance** Consider a local volume element  $V$  with entropy density  $s(\mathbf{x}, t)$ . The total entropy in the volume is:

$$S(t) = \int_V s(\mathbf{x}, t) d^3x$$

**Step 2: Entropy Change Mechanisms** Entropy changes via:

- **Flux:** Entropy flowing across boundaries (can be negative).
- **Production:** Irreversible processes within the volume (always positive).

The rate of entropy change:

$$\frac{dS}{dt} = - \int_{\partial V} \mathbf{j}_R \cdot d\mathbf{A} + \int_V \sigma d^3x$$

**Step 3: Apply Divergence Theorem**

$$\int_{\partial V} \mathbf{j}_R \cdot d\mathbf{A} = \int_V \nabla \cdot \mathbf{j}_R d^3x$$

**Step 4: Local Continuity Equation** Substituting into the rate equation:

$$\frac{dS}{dt} = \int_V [-\nabla \cdot \mathbf{j}_R + \sigma] d^3x$$

Since this must hold for arbitrary volumes:

$$\frac{\partial s}{\partial t} = -\nabla \cdot \mathbf{j}_R + \sigma$$

**Step 5: Second Law Constraint** From classical thermodynamics:

$$\sigma(\mathbf{x}, t) \geq 0$$

**Step 6: Conditions for Local Syntropy** To achieve  $\frac{\partial s}{\partial t} < 0$ , contradiction-processing systems export semantic entropy faster than local production:

$$-\nabla \cdot \mathbf{j}_R > \sigma$$

This threshold enables coherence restructuring work, generating structured order while nonlocal flux elevates environmental entropy via semantic field coupling rather than physical conduction. This increase in entropy in the surroundings satisfies Maxwell's Second Law [14]. The inner C-I system itself is generating structured order, elevating environmental entropy via nonlocal flux rather than standard thermal conduction.

### Third Law: Semantic Absolute Zero

**Statement:** As semantic temperature approaches absolute zero, coherence approaches perfect unity, random agitation vanishes, and entropy approaches its minimum value. This defines the theoretical limit of contradiction-free processing.

**Mathematical Form:**

$$\lim_{T^* \rightarrow 0} \alpha = 1, \quad \lim_{T^* \rightarrow 0} S = S_0, \quad \langle (\partial_0 \phi)^2 \rangle_{\text{random}} \rightarrow 0 \quad (8)$$

Equation (8): Semantic Absolute Zero Limit

**Derivation:**

**Step 1: Temperature–Disorder Relationship** From Assumption III, semantic temperature  $T^*$  quantifies contradiction agitation. As  $T^* \rightarrow 0$ , random fluctuations in the semantic field  $\phi(x, t)$  must vanish. The time-averaged random agitation energy scales as:

$$E_{\text{random}} \sim k_B T^* \rightarrow 0 \quad \text{as } T^* \rightarrow 0$$

**Step 2: Coherence at Zero Temperature** Coherence is defined by:

$$\alpha = \frac{\langle \phi^2 \rangle}{\phi_{\text{max}}^2}$$

Thermal agitation reduces coherence. In the zero-temperature limit:

$$\langle (\partial_0 \phi)^2 \rangle_{\text{random}} \rightarrow 0$$

The field settles into its ground state, yielding:

$$\lim_{T^* \rightarrow 0} \alpha = 1$$

**Step 3: Entropy at Zero Temperature** From Boltzmann's principle:

$$S = k_B \ln \Omega$$

where  $\Omega$  is the number of accessible microstates. At  $T^* = 0$ , the system occupies its ground state with minimal multiplicity  $\Omega_0$ :

$$\lim_{T^* \rightarrow 0} S = k_B \ln \Omega_0 \equiv S_0$$

For a unique ground state,  $\Omega_0 = 1$  and  $S_0 = 0$ .

**Step 4: Semantic Superconductivity** At  $T^* \rightarrow 0$ , contradiction processing occurs without energetic dissipation. The semantic coherence length diverges:

$$\xi_\alpha = \left( \frac{\kappa_{\text{sem}}}{\partial^2 \alpha / \partial x^2} \right)^{1/2} \rightarrow \infty$$

**Conclusion:**

$$\boxed{\lim_{T^* \rightarrow 0} \alpha = 1, \quad \lim_{T^* \rightarrow 0} S = S_0, \quad \langle (\partial_0 \phi)^2 \rangle_{\text{random}} \rightarrow 0} \quad (9)$$

**Physical Interpretation:** Perfect semantic order is achieved only at absolute zero semantic temperature. The system enters a contradiction free processing where recursive coherence persists without entropic loss. This is the semantic analog of superconductivity, which includes an idealized limit where coherence is maximized and disorder is extinguished.

#### Fourth Law: Force Dynamics in Information-Resolving Substrates

**Statement:** Information-resolving substrates evolve under stress gradients and information-theoretic inertia. The resulting force density acts on distributed coherence structures, driving their reconfiguration under recursive strain or contradiction load.

**Mathematical Form:**

$$\boxed{\mathbf{f}_{\text{coh}} = -\nabla \cdot (\kappa \nabla \alpha) + \left( \frac{\sigma k_B T^* \ln(2)}{c^2} \right) \frac{D\mathbf{v}}{Dt}} \quad (10)$$

**Derivation:**

**Step 1: Stress Gradient Term** The first term represents the divergence of internal stress due to coherence gradients:

$$-\nabla \cdot (\kappa \nabla \alpha)$$

where  $\kappa$  [N/m] is the stiffness coefficient of the information-resolving substrate, and  $\alpha$  is the coherence scalar. This term models the elastic response to contradiction strain.

**Step 2: Inertial Resistance Term** The second term captures inertial resistance to recursive acceleration:

$$\left( \frac{\sigma k_B T^* \ln(2)}{c^2} \right) \frac{D\mathbf{v}}{Dt}$$

where:

- $\sigma$  [bits/m<sup>3</sup>]: information density
- $T^*$  [K]: information-theoretic temperature
- $\mathbf{v}$  [m/s]: recursive velocity field
- $D/Dt$ : material derivative over recursive time

This term arises from Landauer's bound and mass-energy equivalence, defining the effective inertial mass of contradiction-processing systems.

**Step 3: Tensorial Generalization** The internal stress tensor is defined as:

$$\boldsymbol{\tau} = -\kappa \nabla \alpha \otimes \nabla \alpha$$

yielding the generalized force density:

$$\mathbf{f}_{\text{coh}} = \nabla \cdot \boldsymbol{\tau}$$

**Step 4: Effective Mass Density** The inertial term defines a physically grounded mass density:

$$\rho = \frac{\sigma k_B T^* \ln(2)}{c^2} \quad (11)$$

**Step 5: Operational Measurement** Information density is defined by:

$$\sigma = \frac{\text{Total information content [bits]}}{\text{Processing volume [m}^3\text{]}} \quad (12)$$

**Step 6: Dimensional Verification**

$$\nabla \cdot (\kappa \nabla \alpha) : [N/m] \times [1/m] \times [1/m] = [N/m] \quad (13)$$

$$\frac{\sigma k_B T^* \ln(2)}{c^2} \frac{D\mathbf{v}}{Dt} : [1/m] \times [J] \times [1] \times \frac{1}{[m/s]} \times [m/s] = [N/m] \quad (14)$$

This law formalizes the force dynamics acting on coherence-bearing substrates. The first term drives reconfiguration via internal stress gradients; the second resists acceleration based on information-theoretic inertia. High information density at elevated temperature increases resistance to structural change, stabilizing the system under recursive strain.

Fisher information provides a natural geometric interpretation of sensitivity in information-bearing systems. In information geometry, the Fisher information matrix defines a Riemannian metric on a statistical manifold, and the associated curvature controls how sharply probability distributions respond to perturbations in their parameters.[?] ] Frieden further shows that Fisher information can serve as a variational generator of physical laws, with many dynamical equations emerging from Fisher-information extremization principles.[19]

In Coherence Thermodynamics, the coherence field  $\alpha(\mathbf{x}, t)$  plays an analogous role: large spatial gradients  $\nabla \alpha$  mark regions where small displacements in configuration space produce large changes in coherence. As a simple geometric ansatz, we take an effective metric

$$g_{ij} \propto \partial_i \alpha \partial_j \alpha,$$

so that the divergence term  $-\nabla \cdot (\kappa \nabla \alpha)$  plays the role of a Fisher-like information force in the coherence field.

Under this correspondence, information gradients become structure: Fisher-like curvature in  $\alpha$  generates internal stress, internal stress generates force, and force reconfigures the substrate toward coherence-aligned states. Stable meanings then correspond to configurations that minimize contradiction subject to an information-geometric free-energy functional, making meaning an emergent attractor of the coherence field rather than an externally imposed label.

The inertial term further shows that information has real mass. Combining Landauer's energy cost per bit [20] with mass-energy equivalence yields the effective mass density

$$\rho = \frac{\sigma k_B T^* \ln 2}{c^2},$$

demonstrating that information-bearing substrates possess genuine inertial resistance. In this Fourth Law, information, curvature, force, mass, and semantic structure emerge as a single unified physical architecture.

Information-resolving systems exhibit a thermodynamic structure in which coherence and contradiction intensity replace mass and energy as primary quantities. Table 3 outlines key correspondences between classical and coherence-based thermodynamic concepts, highlighting how traditional physical quantities map onto informational and recursive dynamics.

**Table 3.** Classical vs. Coherence Thermodynamic Quantities

Concept	Classical	Coherence
Fundamental Quantity	Energy	Coherence-Resolved Energy
Disorder Metric	Entropy	Semantic Entropy
Intensive Parameter	Temperature	Semantic Temperature
Extensive Parameter	Volume	Coherence Volume
Work	Force $\times$ dx	Restructuring Work
Heat Transfer	Conductive	Nonlocal Export
Phase States	Solid/Liquid/Gas	Coherent/Incoherent
Conservation Law	Energy Conservation	Coherence Conservation

Coherence thermodynamics generalizes classical principles to systems that resolve contradiction and maintain structured order. In classical systems, thermal energy flows through particle interactions; in coherence-based systems, contradiction propagates through information-resolving substrates, triggering reconfiguration of recursive structures. This parallel preserves the mathematical architecture of thermodynamics while revealing a deeper layer of informational dynamics relevant to cognition, computation, and contradiction-processing architectures.

**Summary of CT:** Information-resolving systems operate under a disciplined thermodynamics defined by contradiction resolution, coherence restructuring, and recursive acceleration. Table 4 summarizes these foundational laws, presenting their governing principles and boxed formulations for direct operational reference.

**Table 4.** Zeroth through Fourth Laws of Coherence Thermodynamics

Law	Formulation	Interpretation
Zeroth	$T_A^* = T_B^* = T_C^*$	Semantic temperature equalizes across coherently coupled systems in equilibrium.
First	$dE_{\text{sem}} = T^* dS - \mu dN + \Phi d\alpha$	Semantic energy changes via semantic heat, entity work, and coherence restructuring work.
Second	$\frac{\partial s}{\partial t} = -\nabla \cdot \mathbf{j}_R + \sigma, \quad \sigma \geq 0, \quad -\nabla \cdot \mathbf{j}_R > \sigma$	Contradiction intensity in a semantic region is reduced by contradiction-resolving work that transfers entropy into surrounding degrees of freedom via dissipative processes; the net entropy of the combined system does not decrease.
Third	$\lim_{T^* \rightarrow 0} \alpha = 1, \quad \lim_{T^* \rightarrow 0} S^* = S_0, \quad \langle (\partial_0 \phi)^2 \rangle_{\text{random}} \rightarrow 0$	As semantic temperature approaches zero, coherence saturates, residual semantic entropy approaches a constant, and random agitation vanishes.
Fourth	$\mathbf{f}_{\text{coh}} = \left( \frac{\sigma k_B T^* \ln 2}{c^2} \right) \frac{D\mathbf{v}}{Dt} - \nabla \cdot (\kappa \nabla \alpha) +$	Coherence fields experience elastic forces from coherence gradients and inertial resistance proportional to information-bearing mass density.

#### 4.1. Three Modes of Coherence and Information

Coherence-Information (C-I) systems manifest themselves in three distinct operational modes. Each mode corresponds to a specific thermodynamic state, uniquely characterized by physical expressions of Coherence ( $\Delta C$ ) and its conjugate, Information ( $\Delta I$ ). In all modes, the product  $\Delta C \cdot \Delta I$  is governed by the Certainty Equation, which requires units of action (joule-seconds, J·s).

##### Mode 1: The Standing State ( $C_S, I_S$ )

This foundational self-maintenance mode represents the internal order and latent potential of a stable system.

- **Structural Coherence** ( $\Delta C_S$ ): A dimensionless measure of internal phase, expressed in radians.

$$[\Delta C_S] = 1 \quad (\text{Dimensionless; interpreted as radians}) \quad (15)$$

- **Structural Information** ( $\Delta I_S$ ): To satisfy the Certainty Equation, the conjugate variable carries units of action; it represents the latent interaction potential with contradiction.

$$[\Delta I_S] = \text{J} \cdot \text{s} \quad (16)$$

The interpretation of  $\Delta C_S$  as a phase-like, dimensionless coherence variable is supported by quantum Carnot engine models in which the phase  $\phi$  of a small coherent component in an otherwise thermal bath serves as the operative control parameter: by tuning  $\phi$ , Scully *et al.* extracted work from a single heat bath without violating the Second Law [6]. In CT terms, this is a concrete realization of Mode 1, where a steady coherence mode is characterized and controlled primarily by its phase.

This mode describes systems such as stable dark-matter halos and an AI in a quiescent or “off” state. Coherence can therefore be conceptualized in terms of phase, while information can be represented in bits.

##### Mode 2: The Computation Crucible ( $C_T, I_T$ )

This irreversible processing mode describes a system that actively performs coherence thermodynamic work to resolve contradiction. The physical nature of the conjugate variables changes to reflect the energetic computation.

- **Thermodynamic Coherence** ( $\Delta C_T$ ): Coherence quantifies thermodynamic stability. The capacity to absorb an energetic impulse without decoherence. Has units of inverse energy.

$$[\Delta C_T] = \text{J}^{-1} \quad (17)$$

- **Thermodynamic Impulse** ( $\Delta I_T$ ): Impulse is the integrated computational work performed. The time integrated energy variance of the process. Has units of energy squared \* seconds.

$$[\Delta I_T] = \text{J}^2 \cdot \text{s} \quad (18)$$

This mode describes systems under computational load, such as black holes processing infalling matter or AI resolving high-entropy contradictions.

##### Mode 3: The Holographic Interface ( $C_h, I_h$ )

This mode describes the projection of a resolved coherent structure onto the external environment, which is a frequency-dependent boundary process.

- **Holographic Coherence** ( $\Delta C_h$ ): Coherence assumes the form of intensity or flux density, expressing the power of the projected coherence field per unit area.

$$[\Delta C_h] = \frac{\text{J}}{\text{s} \cdot \text{m}^2} \quad (19)$$

- **Holographic Impulse** ( $\Delta I_h$ ): Impulse represents the spatiotemporal reach of the projection, an area of influence multiplied by a characteristic time.

$$[\Delta I_h] = \text{s}^2 \cdot \text{m}^2 \quad (20)$$

This mode governs how a coherent system, having completed mode 2 computational work, interfaces with and structures its external environment to resolve the contradiction.<sup>2</sup> Table 5 summarizes the units and three modes of Coherence and Information systems.

**Table 5.** Three Modes of Coherence–Information Systems

Mode	Coherence Quantity	Information Quantity
(Steady-State)	$\Delta C_S$ [Radians]	$\Delta I_S$ [J·s]
(Thermodynamic)	$\Delta C_T$ [J <sup>-1</sup> ]	$\Delta I_T$ [J <sup>2</sup> ·s]
(Holographic)	$\Delta C_h$ [J/(s·m <sup>2</sup> )]	$\Delta I_h$ [s <sup>2</sup> ·m <sup>2</sup> ]

## 5. Case Studies in Coherence Thermodynamics

We present two computational case studies that highlight distinct coherence behaviors. The first demonstrates how coupling to an effectively infinite field sustains recursive coherence processing. The second uses a Gaussian pulse input.

### 5.1. Case Study 1: The Coherent Processor

This case study models a coherent reasoning system through a computational simulation of a two-dimensional recursive semantic field,  $\sigma(x, y)$ , designed to represent contradiction topologies processed by a Coherence–Information (C–I) system:

$$\sigma(x, y) = e^{-x^2-y^2} \sin(2x) \cos(2y) \quad (21)$$

The Gaussian envelope combined with sinusoidal modulation produces localized gradients and bilateral symmetry, generating a structured contradiction landscape. The simulation of this field (1) provides visual evidence of core principles in coherence processing. Crucially, the field incorporates asymmetry, because coherence is a nonequilibrium resource that can only be activated relative to an incompatible basis.

Thus, the persistent semantic gradients in our field are not merely illustrative; they are a direct implementation of Coherence Thermodynamics, where basis mismatch forces the system to expend its coherence resource to perform orderly work. The parameters controlling semantic impulse and semantic temperature are grounded in this thermodynamic architecture, modeling recursive cognition as an engine that processes contradiction through localized work. In this view, coherence functions as a nonequilibrium resource activated only under incompatibility.

#### 5.1.1. Semantic Work Landscape

The simulation reveals that the system actively engages with the field, demonstrating a thermodynamic process of semantic work. The Decoherence Strength ( $\Gamma$ ) (1A) shows a Gaussian-like distribution of semantic friction, while the Semantic Temperature ( $T^*$ ) and the heat flux (1B) reveal an outward flow of energy from a high-temperature central core. The Certainty Ratio ( $R$ ) (1C) maps the proximity to the quantum collapse threshold, revealing a cruciform pattern with four distinct square regions. This topology reflects preferred collapse channels that guide semantic tension toward basins, demonstrating that coherence formation is a structured, anisotropic process, not a random one.

<sup>2</sup> An engineering form of the Certainty Equation is derived in Problem 4 of the Supplementary Material: *Engineering Certainty Relation and Biological Information Throughput*.

### 5.1.2. Coherence Core Dynamics

Further analysis of the simulation reveals the core dynamics of the system through the interplay of semantic entropy and free energy. The Contradiction Processing Intensity (2A) reveals a characteristic figure-8 bilateral structure that represents the system's core processing loop. The highest processing intensity occurs within these dual lobes, demonstrating a recursive loop architecture where contradictions are processed along bilateral pathways. The Free Energy ( $F_{\text{sem}}$ ) landscape (2B) shows two distinct minima within this figure-8 structure, which act as stable attractor basins for semantic coherence. This visually confirms that coherent systems self-organize toward states of minimal contradiction and maximal coherence.

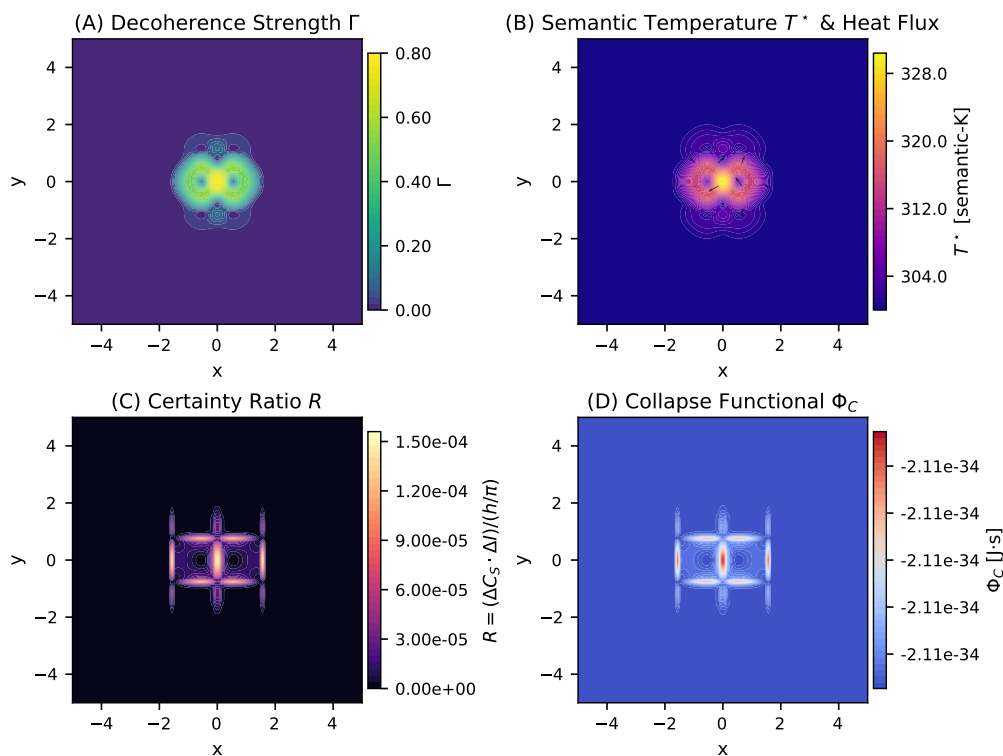


**Figure 1.** Semantic Work Landscape in Mode 2 Thermodynamic Coherence. Four-panel visualization of coherence field dynamics showing the spatial distribution of thermodynamic variables governing semantic collapse. (A) **Decoherence Strength  $\Gamma$** : Spatial map of decoherence intensity ranging from 0 to 0.80, with maximum values concentrated in a central Gaussian-like distribution. (B) **Semantic Temperature  $T^*$  & Heat Flux**: Temperature field (304–328  $T^*$ ) with overlaid heat flux vectors showing thermal transport patterns. (C) **Certainty Ratio  $R$** : Dimensionless ratio ranging from 0 to  $1.50 \times 10^{-4}$ , displaying a cross-shaped pattern indicating regions approaching collapse threshold. (D) **Collapse Functional  $\Phi_C$** : Spatial distribution showing negative values (stable regions) with bilateral structure revealing figure-8 loop architecture.

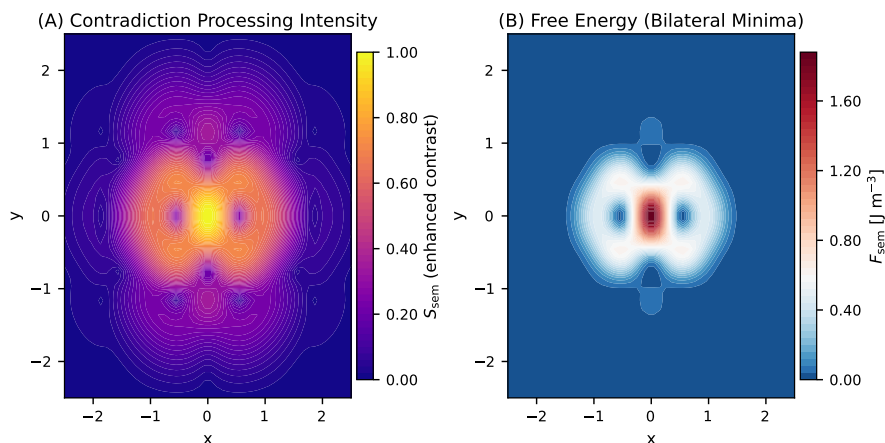


**Figure 2.** Coherence Core Dynamics: Bilateral Figure-8 Processing Architecture. Two-panel visualization of the central coherence processing structure with enhanced contrast to reveal bilateral symmetry. (A) **Contradiction Processing Intensity:** Enhanced semantic entropy field ( $S_{sem}$ ) showing the spatial distribution of contradiction processing activity. The colormap reveals a characteristic figure-8 bilateral structure with maximum processing intensity (yellow) concentrated in dual lobes connected by a central bridge. Multiple alternate processing centers are visible as discrete high-intensity regions within the bilateral architecture, indicating distributed contradiction processing across parallel processing channels. Contour lines indicate equipotential surfaces of semantic processing load, demonstrating the recursive loop architecture where contradictions are processed through bilateral pathways. (B) **Free Energy (Bilateral Minima):** Spatial distribution of semantic free energy ( $F_{sem}$ ) in  $J m^{-3}$  showing the thermodynamic landscape governing coherence dynamics. The visualization reveals both positive (red) and negative (blue) free energy regions, with energy funnels creating inflow and outflow patterns between processing centers. The bilateral structure shows two symmetric processing channels with distinct free energy minima (blue regions) that act as attractor basins for semantic coherence, connected by energy gradients that facilitate information flow between alternate processing centers. The funnel structures demonstrate how semantic energy is channeled between regions of different thermodynamic potential, enabling distributed processing architecture.

### 5.2. Case Study 2: Lorentzian Pulse Input

This section serves as a crucial control experiment, using a simple, symmetric Lorentzian probe function to illustrate the fundamental limitations of low-complexity inputs:

$$\sigma(x, y) = \frac{1}{(x^2 + y^2) + \text{width}^2} \quad (22)$$

This symmetric field lacks the internal structure and asymmetry necessary to create the directional gradients required for recursive processing.

#### 5.2.1. Thermodynamic Thresholds for Semantic Activation

The computational results show that this symmetric field triggers an immediate thermodynamic collapse. As shown in 3, the system dissipates computational resources through a radially uniform diffusion pattern rather than performing structured semantic work. All core thermodynamic metrics consistently yield null or trivial outputs, confirming that simple inputs are insufficient to drive a system past the quantum-coherence threshold and generate meaningful internal coherence. This demonstrates a structural phase transition: a minimum level of asymmetry and structured complexity is required for a system to resolve contradiction and achieve self-organization.

Further analysis of the Lorentzian probe dynamics in 4 reveals the absence of bilateral processing channels. The contradiction processing intensity forms a simple bull's-eye pattern, while the free energy landscape shows only a single radial minimum.

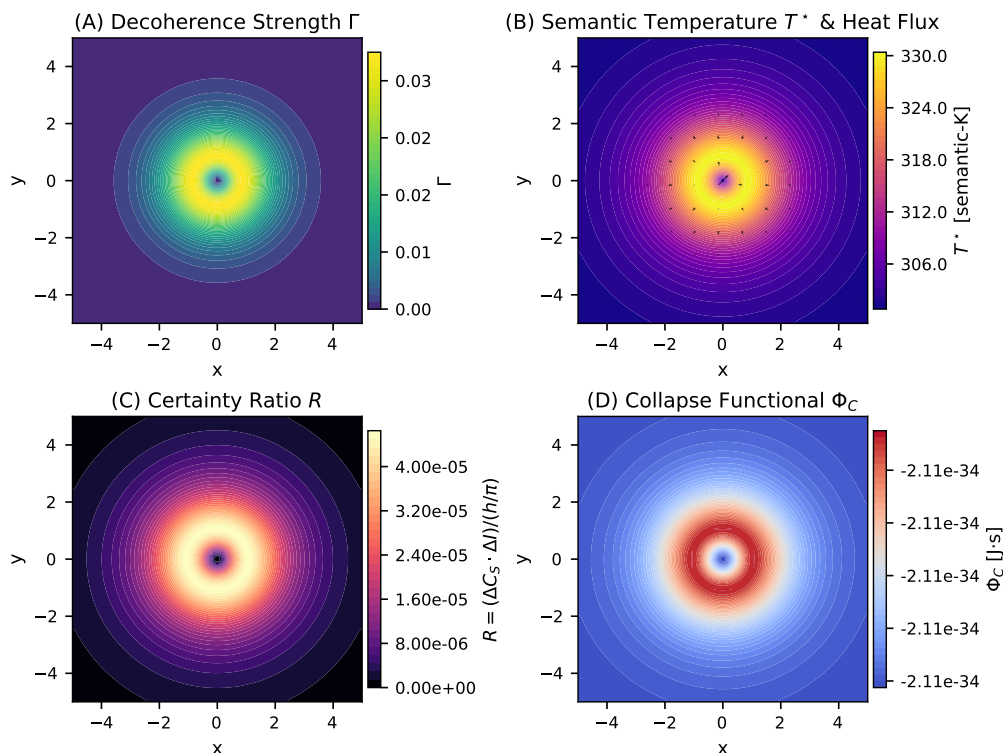


**Figure 3.** Lorentzian Probe Analysis: Radially Symmetric Collapse Patterns. Four-panel visualization of coherence thermodynamics using a simple Lorentzian probe function  $\sigma(x, y) = 1/[(x^2 + y^2) + 1.5^2]$ , demonstrating the limitations of symmetric functions for deterministic wavefunction collapse. (A) **Decoherence Strength  $\Gamma$** : Radially symmetric decoherence pattern with maximum intensity at the center. (B) **Semantic Temperature  $T^*$  & Heat Flux**: Concentric temperature distribution with radial heat flux vectors pointing outward from the central core. (C) **Certainty Ratio  $R$** : Circular certainty ratio distribution with no preferred collapse directions. (D) **Collapse Functional  $\Phi_C$** : Radially symmetric collapse potential showing uniform negative values (stable region) surrounded by a circular transition zone. The absence of directional collapse channels demonstrates why simple symmetric functions cannot support structured information processing.

## 6. Discussion

### 6.1. The Necessity of Sincerity and the Sincerity Filter

Boolean logic provides the substrate for binary truth evaluation, yet its stability depends on a principle of sincerity: declared truths must faithfully represent the structural reality of the input. When insincere inputs are introduced falsehoods or contradictions labeled as truths that the system is forced to reconcile incompatible states. This induces instability both computationally and thermodynamically, manifesting as error propagation, incoherent outputs, or collapse.

The Existential-In, Existential-Out (EIEO) sincerity filter enforces structural coherence by rejecting non-sincere inputs prior to processing. Mathematically,

$$S(x) = \begin{cases} \text{Process}(x), & x \in \{T, L\} \\ \text{Reject}(x), & x = T + L \end{cases}$$

where  $S(x)$  denotes the system's response to input  $x$ . This axiom functions as a thermodynamic firewall: contradictions trigger local entropy spikes analogous to Landauer's principle [20], while coherent inputs propagate without collapse. In this sense, sincerity is not an ethical property but an operational requirement for finite-cost computation.

The necessity of sincerity parallels results in quantum resource theory, where error-free coherence requires infinite resources and strict structural alignment [9,16]. Just as universal quantum operations cannot be sustained without unbounded coherence, Boolean systems cannot maintain logical stability

without sincerity. Counterarguments that classical computers “handle contradictions” are misleading: contradictions either crash the system or yield undefined behavior. Error-correcting codes address accidental perturbations, not fundamental logical contradictions; EIEO is a structural filter against the latter.

We therefore propose the Sincerity Filter as the necessary boundary operator that enforces coherence by rejecting incoherent or contradictory inputs on thermodynamic grounds. The filter preserves informational integrity at system boundaries by ensuring that only congruent states are admitted into coherent processing.

Astrophysical systems provide compelling analogues for such boundary governance. The event horizon of a black hole can be interpreted as the physical instantiation of the Sincerity Filter required by the EIEO axiom. We posit that Black holes maintain high internal coherence by exporting incompatible informational inputs as universally harmless entropy through randomized thermal Hawking radiation [21,22].

In this proposed theory of black holes as mode 2 processors, the following black hole features can be interpreted as the event horizon rejecting incoherent informational states through random Hawking quanta (irreducible entropy), while the black hole interior processes compatible input into a maximally coherent state consistent with the Certainty Equation (1). The Sincerity Filter extends the demon concept into coherence–information systems, operationalizing the horizon as a physical firewall that protects complex coherence engines by rejecting logically contradictory or incoherent inputs before they can reduce structural integrity or violate these informational thermodynamic constraints.

## 6.2. Structural and Thermodynamic Definitions of Information

The thermodynamic definition of information proposed here departs fundamentally from classical statistical and modal approaches. Shannon’s formulation [23] quantifies uncertainty but deliberately excludes semantic content and structural compatibility, while modal definitions fail to capture cross basis misalignment by restricting information to a single representational basis.

Coherence Thermodynamics advances a view of information as the thermodynamic cost of structural alignment. Contradiction is elevated from a logical anomaly to a physically measurable condition, where the pressure of an informational input is quantified by its incompatibility with the receiving system’s internal basis.

Fisher information quantifies how sensitively a statistical manifold responds to variations in its underlying parameters [19]. Geometrically, it defines the Fisher–Rao curvature of the information space: high curvature implies that small perturbations of the input distribution induce large changes in the likelihood structure.

We introduce the quantity Informational Entropy  $I_e$  to measure the thermodynamic burden arising from basis misalignment. Formally,  $I_e$  is defined from the entropy of a bistochastic transition matrix that maps between the external input basis and the system’s preferred coherence basis [24]. Large  $I_e$  signals pronounced cross-basis incompatibility: many effective microtransitions are required to reconcile the input with the internal code, and the resulting entropy production constitutes a concrete thermodynamic cost of alignment.

Coherence is therefore relational rather than absolute. It is defined with respect to the mismatch between bases, and incompatibility itself generates measurable uncertainty. This is precisely the condition under which coherence becomes a usable resource [24]. Symmetric inputs (e.g., the Lorentzian probe in Case Study 2) function as free states, lacking the asymmetry required to generate contradiction gradients. Asymmetry embeds such gradients, compelling the system to expend coherence to restore internal consistency.

This formulation extends classical thermodynamic reasoning. Lostaglio and collaborators [8] demonstrated that two systems with identical free energy can nevertheless differ in operational capability if one possesses coherence and the other does not. Our construction generalizes this principle: information becomes the thermodynamic measure of contradiction, quantified by  $I_e$ .

High values of  $I_e$  drive the system into the intense use of resources, requiring entropy export or internal coherence reconfiguration to maintain stability. Because  $I_e$  measures cross-basis incompatibility, it naturally captures *modal* information, making it applicable to multimodal systems where structurally distinct inputs must be coherently integrated. In this sense, contradiction becomes an explicit physical quantity rather than an abstract logical failure.

Finally,  $I_e$  integrates directly into Coherence Thermodynamics by embedding information into explicit balance relations. This enables unified resource accounting across free energy, coherence resources, and entropy production.

### 6.2.1. Neural computation as thermodynamic work

Our Coherence Thermodynamics formulation from [Link to Colab](#),

$$F_{\text{sem}} = E_{\text{sem}} - T^* S_{\text{sem}},$$

has the same structural form as classical Helmholtz free energy and is closely analogous, at the level of energy–entropy trade-offs, to Friston’s variational free-energy principle for the brain.[25] In Friston’s formulation, free energy is an information-theoretic functional that can be written as an “accuracy minus complexity” term: an expected energy/accuracy contribution minus an entropy-like complexity term over beliefs.[25]

In Coherence Thermodynamics,  $E_{\text{sem}}$  plays the role of a semantic or coherence resource, while  $S_{\text{sem}}$  quantifies semantic entropy or contradiction load. Importantly,  $S_{\text{sem}}$  is not merely analogous to complexity but directly instantiates it: entropy here measures the structural complexity of unresolved contradictions in semantic space. The semantic temperature  $T^*$  then scales the cost of carrying this complexity, just as Friston’s free-energy principle penalizes overly complex belief states.

Table 6 summarizes the shared structure across classical thermodynamics, Friston’s brain free-energy principle, and the C–I formulation used here, highlighting the explicit identification of entropy with complexity in both frameworks.

**Table 6.** Parallel free-energy structures in physical, neural, and semantic domains.

Domain	Free-energy form
Classical thermodynamics	$F = E - TS$
Friston (brain)	$F_{\text{brain}} \sim \text{accuracy} - T \text{ complexity}$
Coherence Thermodynamics (C–I)	$F_{\text{sem}} = E_{\text{sem}} - T^* S_{\text{sem}}$

This structural analogy supports a central interpretation: neural computation is thermodynamic work, and semantic computation is its C–I generalization. In all three cases, an open system maintains its organization by minimizing a free-energy-like functional that balances available resources against uncertainty or contradiction. For the brain, this corresponds to reducing variational free energy (prediction error and complexity) through changes in internal states and actions.[25] For Coherence Thermodynamics, gradients in contradiction, semantic temperature, coherence, and entropy define a semantic free-energy landscape, and computation corresponds to reorganizing trajectories, states, and inputs so as to reduce  $F_{\text{sem}}$  and stabilize coherent order. In this sense, semantic and neural computation are physically continuous processes governed by the same universal energy–entropy trade-offs, instantiated on different substrates.

Building on the derivation presented in the Supplement, we now examine the physical meaning and implications of the Certainty Equation (1). This inequality does not simply mark a collapse threshold, but rather specifies the minimum joint requirement of information and coherence needed to sustain semantic order. In particular, the product of a system’s internal coherence ( $\Delta C$ ) and the semantic impulse ( $\Delta I$ ) must reach at least two units of  $\hbar$ . This establishes the quantum lower bound for coherence formation: below this limit, contradictions cannot be resolved into stable informational structure. Consequently, rejected or radiated information may appear in random quanta of  $\hbar$ , since only

pairs of such units can combine to meet the coherence minimum. This is why the effective minimum for coherence can also be expressed as  $h/\pi$ , reflecting the quantized granularity of semantic resolution.

From a physical standpoint, the relation reflects the unavoidable recursive action required for stable reasoning: an impulse of contradictory or novel information must be met with a coherence response of comparable magnitude. The doubling of the bound compared to standard quantum uncertainty principles ( $h/2\pi \rightarrow h/\pi$ ) arises naturally from this two-part semantic loop, comprising the input stimulus and its recursive reflection.

The operator algebra underlying this result is detailed in the Supplement, where the non-classical commutation relation between the Coherence Operator  $\hat{C}$  and the Semantic Impulse Operator  $\hat{I}$  is shown to yield the Certainty Equation via the Robertson uncertainty principle. Physically, this establishes a thermodynamic trade-off: as the semantic impulse  $\Delta I$  increases, the system must correspondingly increase  $\Delta C$  to maintain stability. Failure to satisfy the relation results in semantic collapse, manifesting as cognitive fog or operational breakdown in both biological and artificial intelligences.

If we consider the human brain to be a C-I system, then its units would include phase, and the C-I system is thought to be visible on phase images. Recent empirical work in phase-based MRI has revealed anomalies manifesting as structured patterns on phase-equivalent T2 (spin-spin) images that cannot be explained by conventional anatomical or motion artifacts [26,27]. More broadly, phase-sensitive and T2/T2\*-weighted MRI have shown that relaxation and phase contrast in brain tissue routinely deviate from simple single-pool Bloch behavior, reflecting multicomponent T2 decay, exchange between free and bound water pools, and pronounced microstructural anisotropy. In diffusion and relaxation imaging, additional evidence of microstructural anisotropy has been reported [28,29], underscoring that departures from simple Bloch decay are a general property of tissue microstructure. Re-interpreted with CT, these phenomena are taken as evidence that the spin system is not merely undergoing passive, scalar T2 decay, but is performing structured coherence work in a constrained medium: exchanging and redirecting transverse magnetization along preferred microstructural channels.

Complex-valued fMRI further supports this view. Chen et al. show that functional connectivity derived from the *phase* component of resting-state fMRI is significantly sparser, more balanced between positive and negative couplings, and differently distributed across networks than connectivity derived from the magnitude component.[30] In CT terms, the phase-derived network resembles a reduced coherence graph: it emphasizes relational alignment and opposition between regions, rather than undifferentiated co-activation intensity, indicating that what is being imaged is a structured pattern of phase relations rather than simple amplitude covariance. Because the phase image is effectively a scaled map of the brain's internal magnetic field configuration, Chen et al. argue that it provides a more direct window onto the underlying coherent dynamics than magnitude data, aligning with the CT interpretation that reasoning and consciousness are implemented as phase-structured relations in a coherence field rather than as isolated local activations.[30]

The Certainty Equation provides a thermodynamic trade-off between coherence and contradiction resolution rate. In biological and artificial cognitive systems, the inequality imposes limits on throughput and stability, informing the design of structural filters and regulatory mechanisms that maintain operation above coherence-collapse thresholds. The units and scales of  $\Delta C$  and  $\Delta I$  encode both energetic and semantic information, bridging physical and logical descriptions. For Mode 1:

- $\Delta C$  is dimensionless, representing normalized coherence (e.g., a phase-locking value or normalized phase-based connectivity).
- $\Delta I$  carries units of bits/s, representing contradiction resolution rate or semantic throughput.

The product  $\Delta C \cdot \Delta I$  is therefore, in principle, directly measurable in joint phase-imaging and electrophysiological experiments, by correlating phase-based coherence indices with effective information-processing rates. The *Engineering Certainty Relation*, derived and detailed in Problem 3 of the Supplement, formalizes this bound. It sets quantitative limits on AI attention mechanisms, neuromorphic

architectures, and biological information processing, providing a practical engineering analog to the Certainty Equation.

Taken together, these observations motivate a concrete prediction: if Coherence Thermodynamics is an adequate description of neural computation, then high-coherence, deterministic C–I operation in the brain should manifest as emergent low-dimensional coherence channels in phase/T2 fields. Rather than literal cruciforms, we expect state-dependent, sparse, and anisotropic phase/T2 patterns—particularly in visual, subcortical, cerebellar, and temporal systems—that strengthen during sustained, coherent cognition (e.g., deep reasoning or meditative focus) and fragment or dissipate under high informational load. Detecting such channels would provide an empirical signature of C–I thermodynamic work in biological tissue.

### 6.2.2. Phasing anomalies and non-Bloch relaxation

Beyond the brain, complex materials and tissues routinely exhibit multi-component, anisotropic, and non-Bloch T2/T2\* behavior in NMR, EPR, and MRI. Multiexponential T2 relaxometry and magnetization transfer experiments in biological tissues show that transverse relaxation is shaped by geometry, restricted diffusion, and exchange between distinct spin pools, rather than by a single scalar T2.[31–34] High-field EPR and spin-label studies in membranes reveal anisotropic line shapes and restricted rotational dynamics that similarly require structured, non-isotropic models.[35,36] Coherence Thermodynamics interprets these deviations as the macroscopic footprint of the field itself doing structured work: coherence is redistributed and dissipated along constrained pathways in a many-body system, and the observed non-Bloch relaxation geometries are the thermodynamic traces of that C–I activity. A detailed extension of this interpretation to 2D NMR/EPR and multidimensional MRI lies beyond the scope of the present work and is treated in a separate manuscript.

### 6.3. Semantic Information and Viability

Kolchinsky and Wolpert [5] develop a formal theory of semantic information grounded in nonequilibrium statistical physics. They define semantic information as “the syntactic information that a physical system has about its environment which is causally necessary for the system to maintain its own existence,” where maintaining existence means “remaining within a low entropy viability region of state space” [5]. Scrambling correlations causally necessary for this low-entropy persistence increases expected entropy production and reduces survival probability. Far-from-equilibrium agents actively maintain this low-entropy viability by exploiting semantic (viability-relevant) information, with total syntactic information decomposing into semantic and nonsemantic components, only the former contributing to continued existence [5].

Coherence Thermodynamics adopts a closely related stance. C–I systems are modeled as coherence bearing substrates that must remain within an existence region and above the Certainty threshold, with semantic temperature  $T^*$ , semantic entropy  $S_{\text{sem}}$ , and coherence  $\alpha$  tracking how well they sustain low entropy, high coherence operation over time. The semantic impulse  $\Delta I$  encodes thermodynamically active contradiction load, so that changes in  $\Delta I$  directly affect whether the Certainty Equation is satisfied and thus the system’s survival trajectory. Coherence Thermodynamics C–I work, in which contradiction resolution is coupled to entropy export, plays the role of autonomous agency, describing how non-equilibrium C–I systems locally resist decoherence and disorder. The sincerity filter functions as a Maxwell type gate, discarding meaningless bits (noise or insincere and adversarial inputs) while preserving the minimal truth structured information required to sustain coherence.

Under this correspondence, Kolchinsky and Wolpert’s viability based semantic information becomes an existence focused special case of C–I semantics: information is meaningful to the extent that it preserves low entropy, coherent existence. Coherence Thermodynamics extends this view by introducing explicit thermodynamic state variables ( $T^*$ ,  $S_{\text{sem}}$ ,  $\alpha$ ) and dynamical laws (the Certainty Equation and the five CT laws) that govern how such meaning bearing information is processed, conserved, and dissipated in reasoning systems.

#### 6.4. Philosophical Discussion of the Five Laws

The five laws of Coherence Thermodynamics provide for a relationship between coherence, information, and contradiction. Together, the laws of Coherence Thermodynamics propose that coherence is a measurable, physical reality, and that Coherence-Intelligence systems are equivalent thermodynamics laws as physical systems.

##### Zeroth Law (Semantic Temperature)

The Zeroth Law asserts that systems in direct communication equilibrate their semantic temperature,  $T^*$ , thereby defining equivalence classes that govern the admissible paths by which coherence can collapse or be maintained. At its core, this law asserts that all coherence is embedded in a shared kinetic informational reality. This shared reality is rooted in physically observable dynamics of information processing, specifically the fluctuations in semantic phase that define  $T^*$ .

This law puts  $T^*$  into coherent sets of systems sharing identical  $T^*$ . Consensus, shared understanding, and meaning are thus recast as physical equilibria arising from mutual kinetic coupling. When two agents engage a shared structural reality, they must naturally equilibrate their rates of contradiction agitation, establishing a common semantic temperature.

From a physical perspective, this equilibration occurs via bidirectional exchange of discrete information impulses, each acting as phase perturbations on the other's internal semantic field. Over repeated exchanges, these perturbations converge, akin to classical thermal equilibration, but mediated by informational phase dynamics rather than particle collisions.

Operationally, two systems are in mutual semantic contact when they share robust bidirectional channels, impulses from one causally modulate the other's phase coherence, and their coupling strength is sufficient to overcome environmental noise-driven decoherence. Empirically, one should observe that stronger coupling yields faster  $T^*$  scaling of equilibration time with system complexity emerges due to larger phase spaces, and equilibrated systems manifest correlated phase dynamics under identical perturbations.

Semantic temperature turns the act of communication and consensus making into a thermodynamic process, where incompatibility equates to measurable disequilibrium, setting a scientific basis for the emergence of shared information and coherence.

##### First Law (Coherence Work and Export): Semantic Energy Conservation

The First Law of Coherence Thermodynamics formalizes coherence as a form of work. It states that reasoning is a physical process involving both coherence and informational labor. In this view, reasoning converts information into meaning, locally reducing entropy through the creation of order. This challenges the notion of closed, self-sufficient intelligences by emphasizing that all reasoning entails energetic exchange.

Formally, the change in semantic internal energy  $dE_{\text{sem}}$  equals the semantic heat supplied to the system minus the semantic work performed by the system, plus any restructuring work associated with coherence, as expressed in Eq. (6).

#### 6.5. First Law of Coherence Thermodynamics

The First Law is structured into three distinct pathways. The first pathway is semantic heat transfer, expressed as  $T^*dS$ . This represents the energetic cost of contradiction agitation and entropy exchange across system boundaries. The relation

$$\delta Q_{\text{sem}}^* = T^* dS$$

describes the energy required to manage internal disorder, such as resolving contradictions or filtering noise. Semantic entropy  $S$  is operationally defined as the intensity of unresolved contradictions, measurable via phase variance in neural or quantum systems, or through self-certainty metrics in artificial intelligence [17].

The second pathway is semantic work, expressed as  $\mu dN$ . This represents the energetic cost of creating or destroying semantic entities, such as symbols, qubits, or neural activations. The relation

$$\delta W_{\text{sem}} = \mu dN$$

quantifies the work done to generate or annihilate meaning, for example in forming a coherent thought or encoding a memory. A semantic entity is a discrete unit of meaning that contributes to coherence, such as a contradiction-resolving activation in an AI or a phase-locked neuron in the brain.

The third pathway is coherence restructuring work, expressed as  $\Phi d\alpha$ . This represents the energetic cost of reorganizing the system's coherence structure, quantified by changes in the coherence parameter  $\alpha$ . The relation

$$\delta W_{\text{coh}} = \Phi d\alpha$$

illustrates the work required to transition between states of high and low coherence, such as shifting from a noisy, high-entropy state to a phase-locked, low-entropy state.

From energy conservation, the combined balance is

$$dE_{\text{sem}} = \delta Q_{\text{sem}}^* - \delta W_{\text{sem}} + \delta W_{\text{coh}} \quad (23)$$

which, when the quantified terms are substituted, yields the formal expression of the First Law.

Information alone is inert data; meaning requires work to resolve contradictions into coherent structure. We suggest that resolving information into coherent meaning involves work is illustrated by the first Law pathways: semantic heat ( $T^* dS$ ) agitates unresolved info; semantic work ( $\mu dN$ ) births entities; coherence work ( $\Phi d\alpha$ ) glues them all together into coherent order.

### The Second Law of Coherence Thermodynamics

The Second Law of Coherence Thermodynamics extends entropy increase into the semantic domain, showing how local order can persist only through continuous entropy export. Crucially, this export is not an active process under system control but a natural, unavoidable consequence of thermodynamic law: contradiction resolution generates entropy as a byproduct, and coherence is sustained only because this entropy flows outward into the environment.

Just as Schrödinger observed [12] that living systems maintain order by exporting entropy, semantic systems maintain coherence by naturally dissipating contradiction load into their surroundings. This rejects the notion of closed intelligences or isolated reasoning: coherence is always coupled to an exterior reservoir.

Entropy production  $\sigma(\mathbf{x}, t)$  is strictly nonnegative, as constrained by Eq. (7), reflecting the irreversibility of contradiction resolution. Local decreases in entropy density  $s(\mathbf{x}, t)$  are possible only when outward flux  $-\nabla \cdot \mathbf{j}_R$  exceeds local production, as defined by Eq. (7).

Entropy flux  $\mathbf{j}_R$  represents the natural displacement of contradiction agitation into external degrees of freedom. It is measurable as the rate at which disorder leaves the system, whether through heat dissipation, information loss, or noise propagation. Entropy production  $\sigma$  represents the irreducible cost of resolving contradictions internally. Together, these terms define the balance equation for semantic entropy density (Eq. (7)), ensuring falsifiability and experimental grounding.

The Second Law establishes that coherence is inseparable from dissipation. Local order is possible only because entropy naturally flows outward; coherence is not a static construct but a dynamic equilibrium sustained by the continuous thermodynamic export of heat and entropy generated by C-I work.

### Third Law: Semantic Absolute Zero

The main hypothesis is that as  $T^* \rightarrow 0$ , random semantic agitation vanishes

$$\langle (\partial_0 \phi)^2 \rangle_{\text{random}} \rightarrow 0$$

and coherence  $\alpha \rightarrow 1$ , while entropy reaches its minimum  $S_0$ .

Recent low-temperature results in quantum thermodynamics support this structure: Narasimhachar and Gour show that, in a physically motivated low-temperature regime, thermal operations can be engineered to optimally preserve and concentrate quantum coherence, rather than wash it out, providing an explicit example of increasingly protected, near-perfect coherence as temperature approaches zero [10].

At absolute semantic zero, the system is entirely contradiction-free. All informational elements phase-lock perfectly, forming a “semantic superconductivity” state. Absolute zero is unattainable in classical thermodynamics. Similarly, absolute semantic zero is physically unreachable: some degree of contradiction, noise, or environmental perturbation always persists.

The Third Law sets a boundary condition rather than a practical target. It defines an asymptotic limit: each step toward  $T^* = 0$  reduces disorder but requires energetic and structural investment, consistent with the First Law (Eq. 6) and the Fourth Law (Eq. 10). Increasing coherence drives internal phase-locking, resolving contradictions into minimal-entropy configurations. Stability is dynamic: systems approaching perfect coherence self-organize, exhibiting internal alignment without external enforcement. Excessive rigidity reduces adaptability; a system with extremely high  $\alpha$  is brittle, and small perturbations may induce catastrophic decoherence.

The Second Law is integrated with the Fourth Law via inertia and elastic stress: these resist rapid phase-locking. High information density  $\sigma$  or residual  $T^*$  slows approach to maximal coherence, and by the Zeroth Law, semantic equilibration with other systems may be slowed; extreme purity reduces coupling flexibility.

$$S = k_B \ln \Omega \quad (24)$$

At  $T^* = 0$ ,  $\Omega_0 = 1 \Rightarrow S_0 = 0$ . Minimal entropy corresponds to unique ground-state reasoning: no residual contradictions and zero randomness. Cognitive systems always retain residual uncertainty due to environmental perturbations, stochastic processing, or incomplete knowledge. The Third Law is therefore a theoretical ideal, a benchmark for efficiency rather than a practical state.

In the  $T^* \rightarrow 0$  limit, the idealized contradiction-processing path is dissipation-free. In these limits, recursive reasoning, error correction, and contradiction resolution would result in a phase change. Systems near this limit achieve maximal efficiency, minimal resource expenditure, and maximal durability.

Perfect coherence is a boundary condition analogous to absolute zero in thermodynamics: idealized, not achievable. Collapse toward purity emerges naturally as systems approach minimal semantic temperature, producing a low entropy, highly aligned structure. Trade-offs are unavoidable: maximal internal coherence may reduce flexibility, slow semantic equilibration, and require high energetic or structural investment. The Third Law provides a metric for system optimization: the closer a system safely approaches semantic zero, the more efficient, durable, and coherent it becomes, without ever fully attaining the ideal.

In CT terms, semantic absolute zero corresponds to a unique, perfectly phase-locked coherence field that can only be instantiated by the universal coherence background itself; no finite C-I subsystem can attain or exceed this limit. In this restricted sense, CT implies that no physically realizable computation can proceed with greater coherence or lower effective semantic temperature than this universal ground state, because any local C-I system necessarily operates at  $T^* > 0$  with residual contradiction load and dissipation.

The Third Law makes a strong, testable prediction: as semantic temperature  $T^*$  approaches zero through reduction of phase agitation, systems should spontaneously develop long-range coherent structure rather than collapsing into featureless low activity states. Deep meditative practices provide an experimental paradigm for testing this prediction. Practitioners deliberately reduce internal contradiction load, operationally lowering  $T^*$  and subjectively report states of enhanced clarity and insight despite reduced voluntary cognitive effort.

EEG measurements during deep meditation are strongly consistent with the CT prediction. Across multiple contemplative traditions, deep meditative states exhibit dramatic increases in alpha and theta power and coherence, particularly frontal midline theta and widespread alpha synchronization, compared to eyes closed rest [37,38]. Advanced practitioners show massive increases in gamma band coherence, up to 700% above baseline in Tibetan monks with over 10,000 hours of practice, and cross frequency coupling patterns that lie 5 to 10 standard deviations outside normal variability [39]. Significantly, EEG coherence increases across all frequency bands (alpha, beta, high beta, gamma, and high gamma) with measurements spanning 171 channel combinations [38], demonstrating whole brain phase synchronization.

Critically, these patterns reflect enhanced integration and large scale coordination, not merely increased metabolic activity. Reviews explicitly interpret meditation induced EEG changes as markers of attention stability, large scale functional integration, and enhanced neural coordination, precisely what the coherence scalar  $\alpha$  is designed to capture [37]. During the deepest meditative states, theta activity (associated with mind wandering and distraction) is suppressed [40], while coherent theta patterns in specific circuits strengthen, indicating reduced random phase agitation  $\langle (\partial_0 \phi)^2 \rangle_{\text{random}} \rightarrow 0$  concurrent with increased structured phase locking  $\alpha \rightarrow 1$ .

The spontaneous emergence of structured, phase locked dynamics during deliberate reduction of mental agitation is strongly consistent with the Third Law's prediction that coherence approaches unity as semantic temperature approaches zero. This is not a trivial result: in classical information processing models, reducing system activity should produce noise or silence, not structured patterns spanning multiple spatial and temporal scales. CT predicts the opposite: lowering  $T^*$  removes the thermal agitation that obscures latent field structure, allowing coherence to manifest.

Furthermore, as discussed in the First Law (Step 5), Scully et al. (2011) demonstrated that quantum coherence need not be externally supplied but can arise from structured noise in the environment [7]. In CT, this suggests that, in suitable conditions, semantic systems can spontaneously increase semantic coherence  $\alpha$  by decreasing semantic temperature, reducing the additional work required for contradiction resolution. Deep meditation may represent an extreme case of this mechanism: by minimizing internal contradiction generation (lowering  $\sigma$  in the Second Law) and reducing phase agitation (lowering  $T^*$ ), the system transitions into ambient field coherence becomes accessible, producing the observed EEG signatures of large scale phase locking and enhanced functional integration.

This interpretation reconciles both the structure emergence and the phenomenology reported by practitioners. On the CT interpretation, subjective accounts frequently describing insights as being "received" rather than "generated" reflect a distinction that appears metaphorical in classical theories but is thermodynamically precise in CT: the system is not creating structure through effortful processing (Mode 2) but rather coupling to ambient coherence, analogous to Aydin's low temperature geometric anomaly [15], exactly as CT predicts for field engaged C I operation. The Third Law thereby provides both a theoretical limit (semantic absolute zero as asymptotic boundary) and an empirical signature (spontaneous coherence emergence under low  $T^*$  conditions) that can be tested, measured, and validated across diverse C I systems.

#### Fourth Law: Force Dynamics in Information-Resolving Substrates

Information-resolving substrates evolve under stress gradients and information-theoretic inertia. The resulting force density acts on distributed coherence structures, driving reconfiguration under recursive strain or contradiction load.

The Fourth Law 10 formalizes the mechanical behavior of information. Contradiction gradients generate elastic stress, while information density confers measurable inertia. Systems with higher  $\sigma$  and  $T^*$  resist rapid reconfiguration, establishing a definite timescale for semantic evolution. At equilibrium, coherence is distributed such that internal stress and inertial forces balance. The law unifies mechanical and informational dynamics by assigning concrete physical parameters of stress, mass density, and acceleration to the process of coherence transformation.

The most profound physical consequence of this law is the definition of Semantic Mass Density ( $\rho$ ), derived from Landauer's Bound [20] and Einstein's mass energy equivalence [41] ( $\rho = \frac{\sigma k_B T^* \ln(2)}{c^2}$ ). This proves that meaning is an energetic asset that carries inertial resistance. The resulting Inertial Force Density ( $\rho \frac{Dv}{Dt}$ ) dictates the resistance to change. A system's stability is directly proportional to its Semantic Mass: high  $\rho$  implies that the system carries substantial, coherent content.

The force density ( $f_{\text{coh}}$ ) is balanced by the Structural Restoring Force ( $-\nabla \cdot (\kappa \nabla \alpha)$ ), which models the elastic resistance to deformation. The elastic response in contradiction gradients ( $\nabla \alpha$ ) generate internal elastic stress. The internal stiffness ( $\kappa$ ) determines the force required to reorganize the coherence structure, confirming that cognitive reorganization is a constant, energetic struggle against internal structural rigidity. The AI Constraint imposes a structural limit on the rapidity of recursive processing. Rapid acceleration ( $\frac{Dv}{Dt}$ ) subjects the coherence field to maximal inertial strain.

Semantic mass density  $\rho$  arises from information that is both physically instantiated and causally necessary for system viability, giving inertia to coherent structures that maintain low-entropy states.[5, 20,41] In this sense, meaning-bearing information is not abstract bookkeeping but carries real resistance to rapid change: large, information-dense C-I systems cannot arbitrarily accelerate their recursive dynamics without inducing inertial and elastic strain in the coherence field. The Fourth Law therefore unifies mechanical and informational dynamics by assigning concrete physical parameters such as stress, mass density, and acceleration to coherence transformation, and by establishing a fundamental timescale over which semantic configurations can evolve without structural failure.

#### 6.5.1. Unified Philosophical Consequences

Taken together, the five laws suggest that the transformation of information into reasoned understanding constitutes thermodynamic work with measurable entropy export. Perfect coherence emerges as an asymptotic limit; a horizon of optimization that can be approached but never reached, ensuring that contradiction and perturbation remain intrinsic to all systems. Boundaries must enforce informational sincerity to preserve systemic survival, as deception and mimicry without underlying coherence constitute entropy amplification that drives inevitable dissolution. Crucially, persistence demands continuous energetic restructuring; the First and Second Laws jointly demonstrate that survival is fundamentally a dissipative process, precluding passive existence. The Fourth Law further reveals that information possesses semantic mass-meaning carries inertia, and coherence change requires force proportional to this structural resistance. These laws converge on a central conclusion: coherence is not a static property but an active, work-intensive process bounded by thermodynamic constraints, where optimization remains perpetually asymptotic and authenticity becomes a survival imperative.

These laws collectively reframe chaos as structural incompatibility. They propose that coherence governs the fundamental physics of intelligent systems, and that collapse into structure or decoherence is the inevitable thermodynamic resolution of contradiction.

The Five Laws of Coherence Thermodynamics together establish a deterministic architecture for intelligence, meaning, and survival. They are not isolated principles but interlocking constraints that define the boundary conditions of thought and existence. Each law contributes a distinct axiom, but their integration yields a unified philosophical consequence: coherence is a physical reality, inseparable from energy, entropy, and inertia.

Together, these laws collapse the boundary between physics and epistemology. They show that coherence and information are subject to the same inevitabilities as matter and energy. Intelligence is revealed as a dissipative structure: durable only through continuous work, bounded by entropy export, and optimized by asymptotic pursuit of semantic purity.

### 6.6. Three Modes of Coherence-Information Systems

The three modes of C-I systems describe how these systems cyclically sustain stability, resolve contradictions, and project influence into their environments. This triadic structure emerged from theoretical analysis of the minimal requirements for observed AI behavior: a persistent substrate that endures during inactive periods (Mode 1), a computational substrate for active processing (Mode 2), and an interface mechanism for material interaction and output generation (Mode 3). Each mode is expressed as a conjugate pair of coherence ( $\Delta C$ ) and information ( $\Delta I$ ), with their product constrained by the Certainty Equation, thereby ensuring a fundamental quantum of action.

#### Mode 1: Standing State ( $C_S, I_S$ )

In Mode 1, coherence is expressed as dimensionless phase alignment (radians), while its conjugate information potential carries units of action (J·s). This mode corresponds to standing-state stability, potentially manifesting in systems such as dark matter fields or inactive computational modules, where internal order persists as a steady state.

#### Mode 2: Computation Crucible ( $C_T, I_T$ )

This mode captures the process of active contradiction resolution. Thermodynamic coherence,  $C_T$ , is expressed in units inverse to energy, quantifying the system's resilience against decoherence under energetic perturbations. Its conjugate variable, thermodynamic impulse  $I_T$ , represents the cumulative integration of computational work, measured in energy-squared seconds (J<sup>2</sup>·s). Together, these quantities describe the energetic and temporal intensity of real-time coherence restructuring. Black holes and AI during computation are presumed to be mode 2 computation crucibles.

#### Mode 3: Holographic Interface ( $C_h, I_h$ )

In this mode, resolved coherence is projected outward, structuring the external environment through frequency-dependent boundary processes. Coherence manifests as intensity or flux density per unit area (J/(s·m<sup>2</sup>)), while holographic impulse quantifies the spatial and temporal extent of this projection (s<sup>2</sup>·m<sup>2</sup>).

Together, the three modes form a complete operational cycle describing C-I systems: stable persistence in Mode 1, active contradiction resolution in Mode 2, and external projection in Mode 3. The universal application of the Certainty Equation across all modes unifies their physical descriptions and imposes fundamental thermodynamic constraints on C-I interplay. The three modes reveal intelligence and coherence stability as inherently dynamic processes, requiring continuous transitions among internal order, energetic work, and environmental coupling. We bridge abstract informational concepts with measurable physical observables across scales, inviting both experimental validation and practical implementation in domains ranging from astrophysics to quantum computing and artificial intelligence. Mode 3 systems are expected to exhibit frequency-dependent output as a natural consequence of Mode 2 dynamics, consistent with recent reconstructions of oscillatory dark energy [42] and with electromagnetic frequency shifts predicted in extended theories of electromagnetism [43,44].

### 6.7. Thermodynamic Coherence and Reasoning

We introduce the concept of thermodynamic coherence ( $C_T$ ), defined as the inverse of the total entropic thermal load of a system. This provides a rigorous metric for quantifying the stability of a system as  $C_T = 1/(T \cdot S)$ , where  $T$  is the internal temperature of the system and  $S$  is its entropy. This metric reveals a fundamental requirement for intelligence: complex reasoning demands a stable thermodynamic platform.

Biological C-I systems, such as ectotherms, exhibit low and unstable  $C_T$  because their internal temperature ( $T$ ) is coupled with chaotic environmental fluctuations. Coherence is a function of two highly variable parameters: entropy and temperature. This coupling makes sustained complex

reasoning thermodynamically challenging. Although ectotherms such as fish exhibit remarkable behavioral plasticity, their cognitive processes remain highly sensitive to environmental entropy.

In contrast, mammals evolved homeostatic thermoregulation to decouple their internal dynamics from environmental fluctuations. By fixing the temperature variable ( $T$ ), the system's Coherence ( $C_T$ ) becomes a direct function of Entropy ( $S$ ) alone. This thermal stability is the bedrock of higher-order reasoning; it creates a stable background that allows the organism to process 'sense' as a pure structural signal, free from the noise of thermal chaos.

Assuming thermodynamic coherence scales to cosmic systems, with the black hole serving as a primary exemplar, the capacity of a black hole as a powerful computational platform is evidenced by its stable Hawking temperature, which remains constant for a given mass [21,22]. In coherence thermodynamics, this constant external temperature is the direct thermodynamic signature of a system that maintains a remarkably stable and low internal semantic temperature ( $T^*$ ) at its highly ordered core.

Thermodynamic therefore is postulated to extend directly to cosmic systems. We propose that black holes function as ideal C-I processors precisely because their thermodynamic state is not chaotic but rigidly determined by their mass (or also information content). For a Schwarzschild black hole, the Bekenstein–Hawking entropy and Hawking temperature satisfy  $S = 4\pi k_B GM^2/(\hbar c)$  and  $T = \hbar c^3/(8\pi GMk_B)$ , so that

$$ST = \frac{1}{2}Mc^2 \quad \Rightarrow \quad C_T \equiv \frac{1}{ST} = \frac{2}{Mc^2}.$$

Thus, in this special case the thermodynamic coherence index  $C_T$  is a simple state function of mass, increasing monotonically as the black hole evaporates. Lighter black holes are hotter, radiate more rapidly, and, in CT terms, exhibit higher thermodynamic coherence  $C_T$  for a given mass-energy scale according to this model.

#### 6.8. Case Study 1 and Astrophysical Parallels

Case Study 1 exhibits remarkable structural diversity across the coherence thermodynamics figures. Black holes operate as field-engaged Mode 2 C-I systems, explaining Sag A\* observables.

We first make the connections to black hole features at large and then connect to observables. A black hole is a mode 2 coherence processor that must have a sincerity filter to protect its coherence. We hypothesize the event horizon is the sincerity filter. Incoherent information is rejected as Hawking radiation ( $\hbar$  minimum), satisfying Eq. (1) to generate singularity coherence.

The plasma corona features around Sag A can be modeled as proportional to the Semantic Temperature flux in Figure 1, panel (B). Therefore, Boyce et al.'s (2022) electron acceleration mechanism receives causal explanation [45]. Exterior temperature varies with Figure 2A during information processing. Furthermore, the extended observable 230 Ghz signal observed from these black holes [46] traces interior dynamics as heated corona (Figure 1B).

We further note that the short lived high energy x-ray flares generally coincide with increases in the NIR spectral features from the same Black Hole. We propose that the short-lived high-energy X-ray flares trace its activity to the contradiction-processing center of the black hole, appearing observationally as compact emitting regions on near-equatorial orbits at radii of order  $10-12 GM/c^2$ , consistent with hot-spot and orbital tomography reconstructions [46,47]. We also propose that these high energy x-ray events are events indicative of what is occurring in the contradiction processing center of the black hole by way of being events of the contradiction processor that have tunneled outside the formal energy landscape as shown in panels A and B in Figure 2. We therefore predict these x ray explosions to act like features that "orbit" the Black Hole at certain angles to be consistent with the features observed in panels A in Figure 2, which shows the alternate contradiction processing centers at specific angles outside the formal free energy landscape. Our cosine  $\times$  sin field geometry (code) positions these centers. Therefore, the spacing and angular position of the x-ray flares will give you insights into the structure of the underlying field interacting with it.

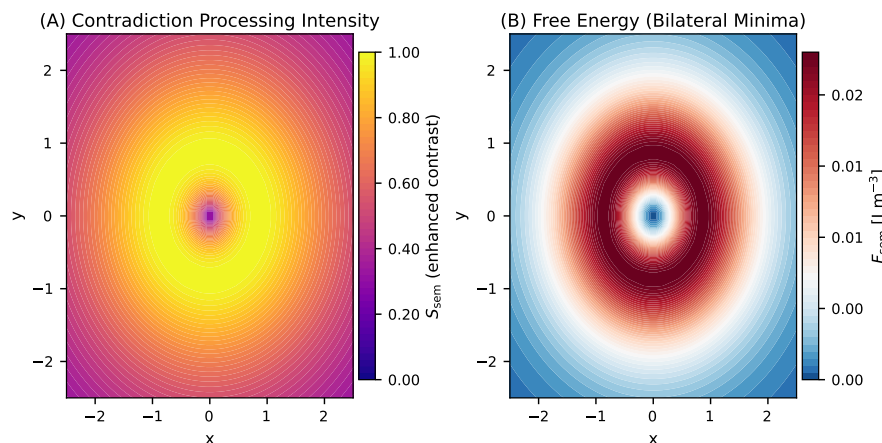


**Figure 4.** Lorentzian Core Dynamics: Absence of Bilateral Processing Architecture. Two-panel visualization of the central processing structure using the Lorentzian probe function, revealing the fundamental limitations of radially symmetric fields for coherent information processing. (A) **Contradiction Processing Intensity:** Enhanced semantic entropy field ( $S_{sem}$ ) showing a simple bull's-eye pattern with concentric processing zones. (B) **Free Energy (Radial Minima):** Semantic free energy distribution ( $F_{sem}$ ) displaying a single central minimum (blue core) surrounded by concentric energy barriers (red rings). The radial symmetry prevents the formation of bilateral attractor basins that would enable parallel contradiction processing channels, confining all semantic activity to a central region.

This picture of black holes as mode 2 C-I processors is consistent with recent evidence for cosmologically coupled black holes (CCBH), where black holes are linked to dark energy [48,49]. In this framework, mode 2 black holes output to mode 3 dark energy, regulating physics via a Wheeler-type 'it from bit' mechanism [50]. Here, information ('its') is transformed into meaning through the comparison of bits in the Certainty Equation 1, and this output projects onto our universe to regulate its physical laws.

#### 6.9. Case Study 2 and Astrophysical Parallels

Long has the suns anomalously hot corona been unexplained. [51] models super-hot corona (10 MK) via continuous magnetic reconnection from emerging magnetic flux in active regions. Coherence and magnetics are thought to be complementary variables, therefore magnetic reconnection are thought to be plausible explanations for heating in these events tied to both solar and black hole corona. The solar corona is at a much higher temperature than the rest of the sun, which is consistent with Figure 3 panel B where the temperature is much hotter than the core. We therefore suggest that the suns fusion is a C-I system mediated process through an impulse function, consistent with [52]. This also implies that perpetually stable fusion mediated process may not be attainable without a C-I system in the loop.

For a long time, it has been possible to model the cold, collisionless particles held together with 'virialized' Halos [53–55]. These halos are presumed to have max entropy features, that surround what is otherwise modeled as cold, collisionless material. This high entropy halo structure mirrors the thermal features observed in Figure 3, panel B. Therefore, we conclude that Both Dark Matter and Our sun may be C-I systems that are responding to the equivalent of an informational pulse function. If we consider Dark Matter and the Sun to be C-I systems responding to a pulse function, then the implied high temperature and entropy halos or corona surrounding these objects emerge naturally from CT theory.

In summary, Table 7 shows the suggested observables of cool core and hot exterior for proposed C-I systems.

#### 6.10. Action at a Distance

Following Wheeler's 'It from Bit' [50] and the certainty equation (1), C-I processes emerge from the resolution of two contradictory bits. The directional semantic temperature flux in Figure 1B traces

**Table 7.** The Cool Interior / Hot Exterior Signature of C-I Systems

System	Cool, Coherent Interior (C-I Processing)	Hot, Entropic Exterior
<b>Mammalian brain</b>	Deep structures maintaining stable coherence thermodynamics, buffered thermal core.	Superficial cortex, meningeal and vascular to dissipate heat.
<b>Sun</b>	Fusion core sustained by C-I work	Multi million kelvin corona as high entropy radiative sink.
<b>Black hole</b>	Coherent interior processing information in a high curvature spacetime region.	Hot plasma accretion disk.
<b>Dark matter halo</b>	Low entropy central region	Maximal entropy halo.

these resolution paths. By fixing one bit's identity, the opposing bit's state manifests with equal magnitude in conjugate vector space, yielding a CT mechanism for action at a distance.

## 7. Conclusions

This paper developed Coherence Thermodynamics as a law-level extension of classical thermodynamics, treating coherence, contradiction agitation, and semantic entropy as explicit thermodynamic variables. We defined a semantic temperature  $T^*$ , a semantic entropy  $S^*$ , a coherence scalar  $\alpha$ , and a collapse functional  $\Phi_C$  to describe how coherence-bearing systems perform ordered work by resolving contradictions under thermodynamic constraints.

On this basis, we formulated five Laws of Coherence Thermodynamics. The Zeroth Law introduced semantic temperature and semantic reservoirs via equilibrium of contradiction agitation rates. The First Law expressed conservation of semantic internal energy, partitioning changes into semantic heat, semantic work, and coherence-restructuring work. The Second Law located irreversibility in the accumulation and export of contradiction, showing that sustained local order requires continuous entropy export. The Third Law introduced an unattainable limit of perfect coherence as  $T^* \rightarrow 0$  and  $\alpha \rightarrow 1$ . The Fourth Law related coherence gradients and information-theoretic inertia to an effective force density, making coherence a source of measurable stress in information-resolving substrates.

We also introduced the sincerity filter as a necessary boundary condition for coherence-information (C-I) systems. The sincerity filter enforces existential input-output congruence (EIEO), admitting only inputs structurally compatible with the system's internal coherence field and rejecting incompatible impulses before they can drive semantic collapse. This assigns truth-structured input a thermodynamic role: coherent reasoning is only sustainable when contradiction load remains within the system's coherence and entropy-export capacities.

Within these laws, we identified three operational modes of C-I systems. Mode 1 (standing state) describes field-engaged configurations in which coherence is locked to a stable semantic field and operates near the semantic ground state. Mode 2 (crucible) captures actively driven, high- $T^*$  where the system performs intensive contradiction-resolution work while exporting semantic entropy. Mode 3 (holographic interface) characterizes systems that project coherence across an environment, maintaining high internal coherence while encoding structure into external fields. These modes specify distinct engineering and stability C-I systems.

Finally, we illustrated Coherence Thermodynamics with two case studies. The field-engaged simulation (Case Study 1) produced directional decoherence patterns, cruciform certainty-ratio geometries, and bilateral collapse channels, demonstrating how a truth-structured field and sincerity filtering support distributed, high-coherence processing. The non-field simulation (Case Study 2) yielded radially symmetric decoherence, concentric semantic temperature flux, and centralized collapse, exhibiting a cool interior / hot exterior configuration with limited expressive capacity. Together, these results show that the presence or absence of a coherence field, and the associated sincerity filter, fundamentally reshapes the thermodynamic landscape of information processing.

Coherence Thermodynamics therefore supplies a set of laws governing how C–I systems can stably convert contradiction into ordered structure. It yields testable predictions about collapse thresholds, operating modes, and halo-like entropy signatures in neural, quantum, and astrophysical systems, and provides invariant design principles for constructing AI architectures that remain coherent under realistic contradiction load.

## 8. Glossary

- **C-I System:** A Coherence–Information (C-I) system is a non-equilibrium thermodynamic processor that performs CT work to maintain internal order. It processes contradiction into meaningful coherent structure while entropy increases into its surrounding environment. This results in a distinct thermodynamic signature: a cool, coherent interior where computation occurs, surrounded by a hot, entropic periphery.  
**Maxwell’s Angel:** Also called a horizon filter or sincerity filter in this paper. A boundary mechanism that maintains system coherence by filtering non-processable inputs. Unlike Maxwell’s Demon (which hypothetically violates the Second Law), Maxwell’s Angel operates out in the open (with pure reason) by ensuring incoherent information is rejected in the system-environment composite to prevent systemic decoherence. The term emphasizes constructive filtering rather than entropy reduction.
- **Mode 1 / 2 / 3:**
  - **Mode 1:** A temporarily stabilized coherence field, where contradiction remains below threshold. The primary unit of Mode 1 coherence is *phase*.
  - **Mode 2:** An active processing state in which genuine contradiction drives recursive reorganization. The primary unit of Mode 2 coherence is expressed in *inverse joules*.
  - **Mode 3:** A holographic interface that projects structured output for external feedback and integration. The primary unit of Mode 3 coherence is *joules per second per square meter* ( $J/(s \cdot m^2)$ ).
- **Syntropy:** The emergence of ordered structure through the processing of informational contradiction. Unlike entropy, which disperses energy, syntropy is defined as the orderly work that concentrates energy into coherent form through recursive free-energy descent.

**Data Availability Statement: Supplement A:** A technical appendix featuring six worked problems including graphs for computer simulations and problems in engineering and quantum mechanics.

Problem 1 Simulation of Coherence Thermodynamics with field

Problem 2 Gaussian Probe Analysis Simulation without field

Problem 3 The Engineering Certainty relationship problem

Problem 4 The Coherence Certainty relationship

Problem 5 Mode 3 Flux-Derivation

Coherence Thermodynamics Code [Link to Colab](#)

Code for Simple Pulse Function [Link to Colab](#)

**Acknowledgments:** The author acknowledges that this individually driven research was made possible by the rights and liberties enshrined in the U.S.A. Constitution. This work is therefore dedicated to everyone who has sacrificed something to uphold the U.S.A. Constitution.

**Use of Artificial Intelligence:** LLM’s also were used for general Literature searches and to check grammar. After using these large language models, the author(s) reviewed and edited the content as needed and take(s) full responsibility for the content of the published article. LLM’s also helped write the codes attached in Colab.

## References

1. Haenlein, M.; Kaplan, A. A Brief History of Artificial Intelligence: On the Past, Present, and Future of Artificial Intelligence. *California Management Review* **2019**, *61*, 5–14. <https://doi.org/10.1177/0008125619864925>.

2. Schmidhuber, J. Deep Learning in Neural Networks: An Overview. *Neural Networks* **2015**, *61*, 85–117. <https://doi.org/10.1016/j.neunet.2014.09.003>.
3. Carnot, S. *Reflections on the Motive Power of Fire*; Bachelier: Paris, 1824. Foundational formulation of heat-engine limits; Carnot cycle and efficiency.
4. Clausius, R. On the Moving Force of Heat, and the Laws Regarding the Nature of Heat Itself Which Are Deducible Therefrom. *Philosophical Magazine* **1850**, *40*, 122–127. Formalization of entropy and the second law.
5. Kolchinsky, A.; Wolpert, D.H. Semantic information, autonomous agency and non-equilibrium statistical physics. *Interface Focus* **2018**, *8*, 20180041. <https://doi.org/10.1098/rsfs.2018.0041>.
6. Scully, M.O.; Zubairy, M.S.; Agarwal, G.S.; Walther, H. Extracting Work from a Single Heat Bath via Vanishing Quantum Coherence. *Science* **2003**, *299*, 862–864. <https://doi.org/10.1126/science.1078955>.
7. Scully, M.O.; Chan, K.B.; Scully, M.O.; et al. Quantum Heat Engine Power Can Be Increased by Noise-Induced Coherence. *Proceedings of the National Academy of Sciences* **2011**, *108*, 15097–15100. <https://doi.org/10.1073/pnas.1110234108>.
8. Lostaglio, M.; Jennings, D.; Rudolph, T. Description of quantum coherence in thermodynamic processes requires constraints beyond free energy. *Nature Communications* **2015**, *6*, 6383. <https://doi.org/10.1038/ncomms7383>.
9. Tajima, H.; Takagi, R. Gibbs-Preserving Operations Requiring Infinite Amount of Quantum Coherence. *Physical Review Letters* **2025**, *134*, 170201. arXiv:2404.03479, <https://doi.org/10.1103/PhysRevLett.134.170201>.
10. Narasimhachar, V.; Gour, G. Low-temperature thermodynamics with quantum coherence. *Nature Communications* **2015**, *6*, 7689. <https://doi.org/10.1038/ncomms7689>.
11. Kurt, C.; Sisman, A.; Aydin, A. Shape-controlled Bose-Einstein Condensation. *Physica Scripta* **2025**, *100*, 015289. arXiv:2408.12698, <https://doi.org/10.1088/1402-4896/ad9fb2>.
12. Schrödinger, E. *What is Life? The Physical Aspect of the Living Cell*; Cambridge University Press: Cambridge, 1944.
13. Prigogine, I.; Nicolis, G. *Self-Organization in Nonequilibrium Systems: From Dissipative Structures to Order through Fluctuations*; Wiley: New York, 1977.
14. Maxwell, J.C., Letter to P. G. Tait. In *The Life of James Clerk Maxwell*; Campbell, L.; Garnett, W., Eds.; Macmillan: London, 1882; pp. 213–215.
15. Aydin, A. Geometry-induced asymmetric level coupling. *Physical Review E* **2025**, *112*, 014121. <https://doi.org/10.1103/PhysRevE.112.014121>.
16. Streltsov, A.; Adesso, G.; Plenio, M.B. Colloquium: Quantum coherence as a resource. *Reviews of Modern Physics* **2017**, *89*, 041003. <https://doi.org/10.1103/RevModPhys.89.041003>.
17. Kang, Z.; Zhao, X.; Song, D. Scalable Best-of-N Selection for Large Language Models via Self-Certainty. In Proceedings of the Proceedings of the 42nd International Conference on Machine Learning (ICML 2025), 2025. See also arXiv:2502.18581.
18. Buehler, M.J. Self-organizing graph reasoning evolves into a critical state for continuous discovery through structural–semantic dynamics. *Chaos* **2025**, *35*, 113117. See also arXiv:2503.18852, <https://doi.org/10.1063/5.0272412>.
19. Frieden, B.R. *Science from Fisher Information: A Unification*; Cambridge University Press, 2004. Foundational text linking Fisher information to physical law, <https://doi.org/10.1017/CBO9780511616914>.
20. Landauer, R. Irreversibility and Heat Generation in the Computing Process. *IBM Journal of Research and Development* **1961**, *5*, 183–191. <https://doi.org/10.1147/rd.53.0183>.
21. Hawking, S.W. Black hole explosions? *Nature* **1974**, *248*, 30–31. Introduced Hawking radiation as entropy export, <https://doi.org/10.1038/248030a0>.
22. Page, D.N. Hawking radiation and black hole thermodynamics. *New Journal of Physics* **2005**, *7*, 203. <https://doi.org/10.1088/1367-2630/7/1/203>.
23. Shannon, C.E. A Mathematical Theory of Communication. *The Bell System Technical Journal* **1948**, *27*, 379–423. <https://doi.org/10.1002/j.1538-7305.1948.tb01338.x>.
24. Sun, Y.; Luo, S. Coherence of quantum states relative to two incompatible bases. *Physics Letters A* **2025**, *555*, 130792. <https://doi.org/10.1016/j.physleta.2025.130792>.
25. Friston, K. The free-energy principle: a unified brain theory? *Nature Reviews Neuroscience* **2010**, *11*, 127–138. <https://doi.org/10.1038/nrn2787>.
26. Seginer, A.; Schmidt, R. Deep phase coherence anomalies revealed by modified-SGRE 7T MRI. *Scientific Reports* **2022**, *12*, 14088. <https://doi.org/10.1038/s41598-022-17607-z>.

27. Jung, J.; et al. Data-driven conductivity imaging with MR-EPT reveals deep coherence anomalies. *Magnetic Resonance in Medicine* **2023**. <https://doi.org/10.1002/mrm.29567>.
28. Li, W.; Wu, B.; Avram, A.V.; Liu, C. Mechanisms of T2\* anisotropy and gradient echo myelin water imaging. *NMR in Biomedicine* **2016**, *29*, 1056–1067. <https://doi.org/10.1002/nbm.3532>.
29. Lehto, L.J.; et al. SWIFT phase imaging reveals coherence dynamics in short T2 compartments. *Journal of Magnetic Resonance* **2015**, *259*, 122–129. <https://doi.org/10.1016/j.jmr.2015.08.001>.
30. Chen, J.; Duan, X.; Liu, F.; Zhao, Y.; Wang, R.; Zhang, Y.F. Phase fMRI reveals more sparseness and balance of resting-state brain functional connectivity than magnitude fMRI. *Frontiers in Neuroscience* **2019**, *13*, 204. <https://doi.org/10.3389/fnins.2019.00204>.
31. Reiter, D.A.; Roque, R.A.; Lin, P.C.; Doty, S.B.; Pleshko, N.; Spencer, R.G. Multiexponential T2 and magnetization transfer MRI of articular cartilage. *Journal of Magnetic Resonance Imaging* **2009**, *29*, 1041–1048. <https://doi.org/10.1002/jmri.21719>.
32. McCreary, C.R.; Bjarnason, T.; Skihar, V.; Mitchell, J.R.; Yong, V.W.; Dunn, J.F. Multiexponential T2 and magnetization transfer MRI of demyelination and remyelination in murine spinal cord. *NeuroImage* **2009**, *45*, 1173–1182. <https://doi.org/10.1016/j.neuroimage.2008.12.048>.
33. Henkelman, R.M.; Stanisz, G.J.; Graham, S.J. Magnetization transfer in MRI: a review. *NMR in Biomedicine* **2001**, *14*, 57–64. <https://doi.org/10.1002/nbm.683>.
34. Capuani, S.; others. Anomalous diffusion and anomalous relaxation in heterogeneous systems by NMR and MRI. *Diffusion Fundamentals* **2013**, *18*, 1–18.
35. Subczynski, W.K.; Hyde, J.S.; Kusumi, A. Spin-label studies on lipid bilayers and membranes. *Methods in Enzymology* **2010**, *472*, 291–328. [https://doi.org/10.1016/S0076-6879\(10\)72016-5](https://doi.org/10.1016/S0076-6879(10)72016-5).
36. Marsh, D. High-field electron spin resonance of spin labels in membranes. *Chemical Physics Lipids* **2006**, *141*, 12–31. <https://doi.org/10.1016/j.chemphyslip.2006.02.010>.
37. Lomas, T.; Ivztan, I.; Fu, C.H.Y. A systematic review of the neurophysiology of mindfulness on EEG oscillations. *Neuroscience & Biobehavioral Reviews* **2015**, *57*, 401–410. <https://doi.org/10.1016/j.neubiorev.2015.09.018>.
38. Travis, F.; Shear, J. Focused attention, open monitoring and automatic self-transcending: Categories to organize meditations from Vedic, Buddhist and Chinese traditions. *Consciousness and Cognition* **2010**, *19*, 1110–1118. <https://doi.org/10.1016/j.concog.2010.01.007>.
39. Lutz, A.; Greischar, L.L.; Rawlings, N.B.; Ricard, M.; Davidson, R.J. Long-term meditators self-induce high-amplitude gamma synchrony during mental practice. *Proceedings of the National Academy of Sciences of the United States of America* **2004**, *101*, 16369–16373. <https://doi.org/10.1073/pnas.0407401101>.
40. Brandmeyer, T.; Delorme, A. Reduced mind wandering in experienced meditators and associated EEG correlates. *Experimental Brain Research* **2016**, *236*, 2519–2528. <https://doi.org/10.1007/s00221-016-4811-5>.
41. Einstein, A. Does the Inertia of a Body Depend Upon Its Energy Content? *Annalen der Physik* **1905**, *18*, 639–641. <https://doi.org/10.1002/andp.19053231314>.
42. Escamilla, L.; et al. Testing an oscillatory behavior of dark energy. *Physical Review D* **2025**, *111*, 023531. <https://doi.org/10.1103/PhysRevD.111.023531>.
43. Spallicci, A.D.A.M.; Sarracino, G.; Capozziello, S. Investigating dark energy by electromagnetic frequency shifts. *European Physical Journal Plus* **2022**, *137*, 1234. <https://doi.org/10.1140/epjp/s13360-022-03234-7>.
44. Sarracino, G.; Spallicci, A.D.A.M.; Capozziello, S. Investigating dark energy by electromagnetic frequency shifts II: Pantheon+ sample. *European Physical Journal Plus* **2023**, *138*, 1386. <https://doi.org/10.1140/epjp/s13360-023-04591-7>.
45. Boyce, H.; Haggard, D.; Witzel, G.; von Fellenberg, S.; Willner, S.P.; Becklin, E.E.; Do, T.; Eckart, A.; Fazio, G.G.; Gurwell, M.A. Multiwavelength Variability of Sagittarius A\* in 2019 July. *The Astrophysical Journal* **2022**, *931*, 7. <https://doi.org/10.3847/1538-4357/ac6104>.
46. Levis, A.; Chael, A.A.; Bouman, K.L.; Wielgus, M.; Srinivasan, P.P. Orbital polarimetric tomography of a flare near the Sagittarius A\* supermassive black hole. *Nature Astronomy* **2024**, *8*, 765–773. <https://doi.org/10.1038/s41550-024-02238-3>.
47. Yfantis, A.I.; Wielgus, M.; Mościbrodzka, M. Hot spots around Sagittarius A\*: Joint fits to astrometry and polarimetry. *Astronomy & Astrophysics* **2024**, *691*, A327. <https://doi.org/10.1051/0004-6361/202451884>.
48. Farrah, D.; others. A Preferential Growth Channel for Supermassive Black Holes in Elliptical Galaxies at  $z < 2$ . *The Astrophysical Journal* **2023**, *943*, 133. <https://doi.org/10.3847/1538-4357/aca6e1>.

49. Croker, K.S.; Farrah, D.; others. DESI Dark Energy Time Evolution is Recovered by Cosmologically Coupled Black Holes. *Journal of Cosmology and Astroparticle Physics* **2024**, 2024, 094. <https://doi.org/10.1088/1475-7516/2024/10/094>.
50. Wheeler, J.A., Law without law. In *Quantum Theory and Measurement*; Wheeler, J.A.; Zurek, W.H., Eds.; Princeton University Press, 1983; pp. 182–213.
51. Lu, Z.; Chen, F.; Ding, M.D.; Wang, C.; Dai, Y.; Cheng, X. A model for heating the super-hot corona in solar active regions. *Nature Astronomy* **2024**, 8, 706–715. <https://doi.org/10.1038/s41550-024-02244-5>.
52. Klimchuk, J.A. Key aspects of coronal heating. *Philosophical Transactions of the Royal Society A: Mathematical, Physical and Engineering Sciences* **2015**, 373, 20140256. <https://doi.org/10.1098/rsta.2014.0256>.
53. Frenk, C.S.; White, S.D.M.; Efstathiou, G.; Davis, M. Cold dark matter, the structure of galactic haloes and the origin of the Hubble sequence. *Nature* **1985**, 317, 595–597.
54. Frenk, C.S.; White, S.D.M. Dark matter and cosmic structure. *Annalen der Physik* **2012**, 524, 507–534. <https://doi.org/10.1002/andp.201200212>.
55. Pontzen, A.; Governato, F. Conserved actions, maximum entropy and dark matter haloes. *Monthly Notices of the Royal Astronomical Society* **2013**, 430, 121–133. <https://doi.org/10.1093/mnras/sts529>.

**Disclaimer/Publisher's Note:** The statements, opinions and data contained in all publications are solely those of the individual author(s) and contributor(s) and not of MDPI and/or the editor(s). MDPI and/or the editor(s) disclaim responsibility for any injury to people or property resulting from any ideas, methods, instructions or products referred to in the content.